



Cite this: *RSC Adv.*, 2024, **14**, 27394

## BrSPR-20-P1 peptide isolated from *Brevibacillus* sp. developed into liposomal hydrogel as a potential topical antimicrobial agent

Narumon Changsan, <sup>a</sup> Apichart Atipairin, <sup>bc</sup> Pajaree Sakdiset, <sup>bc</sup> Poowadon Muenraya, <sup>bc</sup> Neelam Balekar, <sup>d</sup> Teerapol Srichana, <sup>e</sup> Rutthapol Sritharadol, <sup>f</sup> Suranate Phanapithakkun <sup>bc</sup> and Somchai Sawatdee <sup>\*bc</sup>

A novel BrSPR-20-P1 antimicrobial peptide (P1-AMP; NH<sub>2</sub>-VVVNVLVVLPPPVV-COOH) isolated from *Brevibacillus* sp. SPR-20 was encapsulated in a liposome containing varying proportions of L- $\alpha$ -phosphatidylcholine (PC) and cholesterol (CH). P1-AMP liposomes were incorporated into a chitosan hydrogel to achieve a peptide concentration of 0.02%. P1-AMP has been tested for its antibacterial and *in vitro* wound healing activities. The physicochemical characteristics of liposomes and hydrogel were investigated, including *in vitro* drug release, permeability, cell toxicity, antimicrobial activities, and stability studies. P1-AMP showed higher antimicrobial and wound-healing activities than the negative control. A toxicity test of P1-AMP in keratinocyte cell lines revealed cell viability of 100% at a concentration range of 1.96–1000  $\mu$ g mL<sup>-1</sup>. The empty liposomes exhibited an average particle size ranging from 324.5  $\pm$  8.6 to 1823.7  $\pm$  288.2 nm. The size range of P1-AMP liposomes was 378.6  $\pm$  14.0 to 2363.0  $\pm$  255.6 nm. The zeta potential of the blank liposome ranged from  $-40.43 \pm 2.51$  to  $-60.17 \pm 0.93$  mV and it decreased to  $-57.33 \pm 0.72$  to  $-70.33 \pm 0.15$  mV of the liposome loaded with peptide. SEM images showed liposomes were ovoid spheres with smooth surfaces. The chosen formulation, composed of PC to CH in an 18:1 ratio (formulation F3), had the highest entrapment effectiveness with small particle size and possessed an acceptable zeta potential. The developed P1-AMP liposome-loaded hydrogels exhibited a yellowish-clear appearance with a viscosity of 758.0  $\pm$  149.8 cPs. The P1-AMP was rapidly released from the P1-AMP-loaded liposome hydrogel formulation. The P1-AMP-loaded liposome showed high permeability compared to P1-AMP alone or P1-AMP in hydrogel without the incorporation of liposomes. The minimum inhibitory concentration (MIC) against *Staphylococcus aureus* and methicillin-resistant *S. aureus* (MRSA) of P1-AMP-loaded liposome hydrogel was 2  $\mu$ g mL<sup>-1</sup>, equivalent to P1-AMP. It completely killed *S. aureus* at 10 $\times$  and 5 $\times$  MIC after 6 and 12 h of incubation, respectively. The formulation did not induce cytotoxicity to the tested keratinocyte cell and remained stable for at least 6 months under the studied conditions.

Received 20th May 2024  
 Accepted 15th August 2024

DOI: 10.1039/d4ra03722g  
[rsc.li/rsc-advances](http://rsc.li/rsc-advances)

## Introduction

The rise of antibiotic-resistant microorganisms presents a substantial worldwide concern. The recently discovered antimicrobial peptides (AMPs) are fascinating in their potential for fighting antibiotic resistance. Soil bacteria are the primary source of antibiotics. AMPs are a group of molecules produced by *Streptomyces* sp., *Bacillus* sp., and *Brevibacillus* sp. These compounds are effective in combating diseases that have developed resistance to antibiotics.<sup>1,2</sup> AMPs are amphiphilic molecules with a positive charge, typically consisting of 12–50 amino acids, and possess linear motifs such as  $\alpha$ -helix or  $\beta$ -sheet, as well as cyclic or linear configurations.<sup>3</sup> AMPs are essential components of the host's innate immune system, providing protection against a diverse array of pathogens including bacteria, fungi, viruses, and parasites. AMPs exhibit

<sup>a</sup>College of Pharmacy, Rangsit University, Pathumtani, 12000, Thailand. E-mail: [narumon.c@rsu.ac.th](mailto:narumon.c@rsu.ac.th)

<sup>b</sup>School of Pharmacy, Walailak University, Thasala, Nakhon Si Thammarat, 80160, Thailand. E-mail: [apichart.att@mail.wu.ac.th](mailto:apichart.att@mail.wu.ac.th); [pajaree.sa@wu.ac.th](mailto:pajaree.sa@wu.ac.th); [poowadon.me@wu.ac.th](mailto:poowadon.me@wu.ac.th); [suranate.pa@wu.ac.th](mailto:suranate.pa@wu.ac.th); [somchai086@hotmail.com](mailto:somchai086@hotmail.com); [somchai.sa@wu.ac.th](mailto:somchai.sa@wu.ac.th)

<sup>c</sup>Drug and Cosmetics Excellence Center, Walailak University, Thasala, Nakhon Si Thammarat, 80160, Thailand

<sup>d</sup>College of Pharmacy, IPS Academy, Indore, Madhya Pradesh, 452012, India. E-mail: [neelambalekar@gmail.com](mailto:neelambalekar@gmail.com)

<sup>e</sup>Drug Delivery System Excellence Center, Department of Pharmaceutical Technology Faculty of Pharmaceutical Sciences, Prince of Songkla University, Hat Yai, Songkhla, 90112, Thailand. E-mail: [teerapol.s@psu.ac.th](mailto:teerapol.s@psu.ac.th)

<sup>f</sup>Faculty of Pharmaceutical Sciences, Chulalongkorn University, Phaya Thai Road, Pathum Wan, Bangkok, 10330, Thailand. E-mail: [rutthapol.s@chula.ac.th](mailto:rutthapol.s@chula.ac.th)



a wide range of biological roles, such as immunomodulation, angiogenesis, wound healing, and anticancer activity, in addition to their antibacterial capabilities.<sup>4</sup> AMPs are employed by humans as the initial defense against infections and as active agents of the innate immune system.<sup>5</sup> However, AMPs are rarely used in clinical applications due to their short half-life in biological environments like blood.<sup>5</sup>

The novel AMP BrSPR-20-P1 (P1-AMP) has been identified and examined, as demonstrated in Fig. 1.<sup>6,7</sup> Songnaka *et al.* (2022) reported that P1-AMP is composed of 15 amino acids and has the specific structure  $\text{NH}_2\text{-VVVNLVVKVLPPPVV-COOH}$ . The physicochemical properties of P1-AMP are summarized in Table 1. The P1-AMP, isolated from *Brevibacillus* sp. SPR-20, demonstrated significant activity against methicillin-resistant *Staphylococcus aureus* (MRSA) strains and *Staphylococcus aureus*, comparable to that of vancomycin.<sup>7</sup> The physicochemical properties and toxicity of P1-AMP have been studied and reported extensively.<sup>7</sup>

In the case of skin infection, the antimicrobial activity of AMP not only eliminates skin pathogens but also strongly stimulates the host's defense mechanism. Commensal microbes residing on the skin create AMPs that have a direct antimicrobial effect. When harmful microbes are present, the skin's pathogen recognition system is activated, leading to the release of AMPs from keratinocytes.<sup>3</sup> The homeostasis of the skin barrier is actively maintained by these AMP characteristics.<sup>3</sup> Hence, investigating the development of P1-AMP as a topical antimicrobial formulation for the treatment of skin infections and acceleration of wound healing is a topic of interest.

In general, peptides possess relatively large molecules and are naturally unstable, which makes them susceptible to decomposition due to heat, oxidation, and hydrolysis, especially in aqueous solutions.<sup>8</sup> Although the P1-AMP exhibited thermal stability at high temperatures (autoclave), this stability was only maintained for a period of 15 minutes. In addition, P1-AMP demonstrated stability when exposed to proteolytic enzymes, surfactants, and a broad variety of pH values, though only for

a limited duration not exceeding 1 hour.<sup>7</sup> Hence, the application of P1-AMP as an antibacterial agent can be problematic due to its instability when stored for a prolonged period in a pharmaceutical dosage form. Furthermore, AMPs encounter major problems including their ability to permeate to the skin when applied as a topical delivery system.

Liposomes are lipid bilayer structures that can encapsulate both water-soluble and water-insoluble substances. Liposomes are effective for drug delivery, as they can protect encapsulated peptides from degradation, thus enhancing their stability, efficacy, and effective delivery of active chemicals with high entrapment.<sup>9</sup> Furthermore, liposomes possess biocompatibility and the capability to fuse with microbial membranes, rendering them highly efficient for delivering antimicrobial drugs.<sup>10</sup> Additionally, liposomes could serve as a non-toxic penetration enhancer.<sup>11</sup> Liposomes are also utilized in the formulation of wound dressings because of their ability to interact with the structure of the skin and solubilize compounds that have low solubility.<sup>12,13</sup> In addition, the antimicrobial potential of liposomes can be increased by coating their surface and/or adding bioactive compounds. For increasing the stability and improving the shelf life of liposomal products, other compounds such as carbohydrates or protein derivatives could be used within their structure.<sup>12</sup> Some studies fabricated liposomes infused with chitosan to obtain chitosome and encapsulated antibacterial agents. The formulations were safe and exhibited antibacterial activity against positive and/or negative-Gram bacteria.<sup>14,15</sup>

Several researchers have demonstrated the utilization of hydrogel combined with an antibacterial agent for controlled-release applications.<sup>16,17</sup> The incorporation of liposomes into polymeric hydrogel combines the benefits of both drug delivery approaches, resulting in a more advanced method for delivering drugs topically. This approach offers unique advantages, including improved tissue localization, reduced initial release of drugs, and controlled sequential release of drugs.<sup>10</sup>

The present study is the first to exhibit the development of a pharmaceutical dosage form for P1-AMP that enhances the stability and effectiveness of drug delivery to the targeted area while providing ease of application to patients' skin. This work aimed to produce P1-AMP encapsulated liposome-loaded hydrogel that can be easily applied to the skin and has the potential to alleviate infected wounds. The physicochemical characteristics and antibacterial activities were evaluated. In addition, the stability of the selected formulation was assessed to investigate the potential of the P1-AMP formulation to be used in clinical practice.

## Experimental

### Materials

L- $\alpha$ -Phosphatidylcholine (PC), cholesterol (CH), stearylamine, chitosan, and albumin from bovine serum were purchased from Sigma-Aldrich (Darmstadt, Germany). P1-AMP was kindly provided by the laboratory of Dr Apichart Atipairin. Mannitol, glycerol was supplied by P.C. Drug (Bangkok, Thailand). Chitosan (medium molecular weight: 190 000–310 000 Da) was purchased from Sigma-Aldrich (St. Louis, MO, USA).

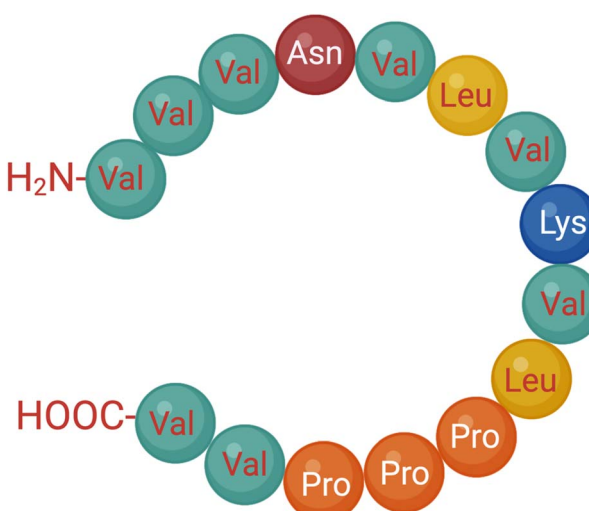


Fig. 1 The primary structure of BrSPR-20-P1 antimicrobial peptide or P1-AMP isolated from *Brevibacillus* sp.



Table 1 Physicochemical properties of P1-AMP<sup>7</sup>

Physicochemical properties	
Mass (Da)	1570.02
Amino acid sequence (N → C)	VVVNVLVKVLPPPVV
Secondary structure (in H <sub>2</sub> O)	α-Helix 4.1% β-Strand 44.0% Turn 19.5% Random 32.4%
Secondary structure (in 50 mM sodium dodecyl sulfate)	α-Helix 25.5% β-Strand 29.3% Turn 10.6% Random 34.6%
Net charge at pH 7.4	+1
Hydrophobicity (H)	0.915
Isoelectric point (pI)	8.62
MIC against <i>S. aureus</i> TISTR 517	2 µg mL <sup>-1</sup>
MIC against MRSA isolate 2468	2 µg mL <sup>-1</sup>

Chloroform and acetic acid were purchased from RCI Labscan (Bangkok, Thailand). Potassium bromide (for IR spectroscopy) was obtained from Loba Chemical Pvt. Ltd. (Mumbai, India). Coomassie Blue G250 was purchased from Bio basic (Markham, Canada). Other chemicals, such as salts used for buffer preparation, were purchased from P.C. Drug (Bangkok, Thailand). Mueller Hinton (MH) and Luria-Bertani (LB) were obtained from Titan Biotech Ltd. (Rajasthan, India). Vancomycin was purchased from Sigma-Aldrich (Co., St. Louis, MO, USA).

### Precipitation and extraction of P1-AMP

The method for the precipitation and extraction of P1-AMP isolated was performed according to previous reports.<sup>6,7</sup> *Brevibacillus* sp. SPR-20 was streaked onto MH agar plates and then incubated in an incubator (Memmert, Incubator, Schwabach, Germany) at 30 °C for 24 h. The inoculated single colony was then diluted with sterile 0.9% NaCl until the optical density (OD) value was 0.1. Subsequently, the resultant was added to an Erlenmeyer flask containing LB broth and then incubated in the shaking incubator (Labtech, Shaking Incubator, Samut Prakan, Thailand) at 30 °C for 24 h. The obtained incubated samples were centrifuged (Sigma Centrifuge 4–16 KS, Osterode, Germany) at 12 000g for 30 min, and the supernatant from the centrifuged samples was precipitated with 75% w/v of ammonium sulfate, which was then centrifuged again at 18 000 rpm for 30 min to obtain the precipitate for dialysis. The obtained peptide products were purified by cation-exchange chromatography, and reverse-phase chromatography was used in the final step of peptide purification. The fraction of P1 obtained was P1-AMP, which was described in a previous study.<sup>7</sup> The schematic preparation of P1-AMP is illustrated in Fig. 2.

### Preliminary testing of antimicrobial activity by the agar well diffusion method

Single colonies of MRSA isolate 2468 were put into a sterile 0.9% NaCl solution. The turbidity was adjusted to an absorbance at 625 nm of 0.1, corresponding to a bacterial density of  $1.5 \times 10^8$  CFU mL<sup>-1</sup>. A sterile cotton swab was dipped in

a turbidity-adjusted MRSA bacterial suspension and spread on the surface of MH agar culture media. A 1000 µL sterile micropipette tip was used to puncture the agar, and then 100 µL of the P1-AMP solution (118 µg mL<sup>-1</sup>) was dropped into the well. The MH media was left at room temperature for 3 h until the sample had completely absorbed in the agar, after which it was incubated at 37 °C for 24 h in the incubator (Memmert Incubator, Schwabach, Germany). Antimicrobial activity was assessed by measuring the diameters of the growth inhibition zones following incubation. All preparations were achieved by using an aseptic technique. All samples were tested in triplicate, and the data were expressed as the mean  $\pm$  standard deviation.

### Protein determination by Bradford protein assay

The Bradford reagent was prepared by dissolving 25 mg of Coomassie Blue G250 in 12.5 mL of 95% ethanol and then adjusting the volume to 50 mL with an 85% (w/v) phosphoric acid solution. After that, the solution was diluted with distilled water to a volume of 250 mL. The Bradford reagent solution was filtered through a 0.45 µm nylon membrane filter and stored at 4 °C until it was used. A standard curve of bovine serum albumin (BSA) was generated by diluting a stock solution of BSA, which had a concentration of 2000 µg mL<sup>-1</sup>, to concentrations ranging from 1 to 100 µg mL<sup>-1</sup> using distilled water. One hundred µL of the P1-AMP was added to 1 mL of Bradford reagent, followed by the addition of 100 µL of 1 M NaOH. The samples were then shaken for 5 minutes, and the absorbance at 595 nm was measured using a UV spectrophotometer (Jasco Corporation, Tokyo, Japan).<sup>18</sup> The obtained values were then used to determine the protein equivalent results.

### Preparation of P1-AMP-loaded liposome

The P1-AMP-loaded liposome comprised lecithin, or L-α-phosphatidylcholine (PC), and cholesterol (CH) in different proportions, as indicated in Table 2. The liposomes were prepared using the lipid thin film hydration technique, as described in the previous literature.<sup>19</sup> Briefly, PC and CH were dissolved in chloroform (10 mL) and transferred to a 100 mL round bottom flask. The chloroform was evaporated using a rotary evaporator (Heidolph HED; Rotary evaporator, Schwabach, Germany) at a speed of 120 rpm with a bath temperature of 40 °C for a duration of 20 min to generate a thin lipid film. The residual chloroform was removed by subjecting the round bottom flask to vacuum pressure for 24 h by using a vacuum oven (WTC Binder GmbH, Tuttlingen, Germany). P1-AMP (100 mg) was dissolved in a 10 mL phosphate buffer saline pH 7.4. The resulting solution was then added to the round bottom flask and gently swirled to hydrate the lipid thin film for 30 min until it was completely released from the round bottom flask wall. The formed liposome vesicle was reduced in size using an ultrasonic bath (Elma E300H, Elma Schmidbauer GmbH, Singen, Germany) at an amplitude of 20 W for 2 hours. Subsequently, a dialysis tube with a molecular weight cutoff of 12 000 Da was used to remove unentrapped P1-AMP from the liposome dispersion system. The resulting P1-AMP liposome



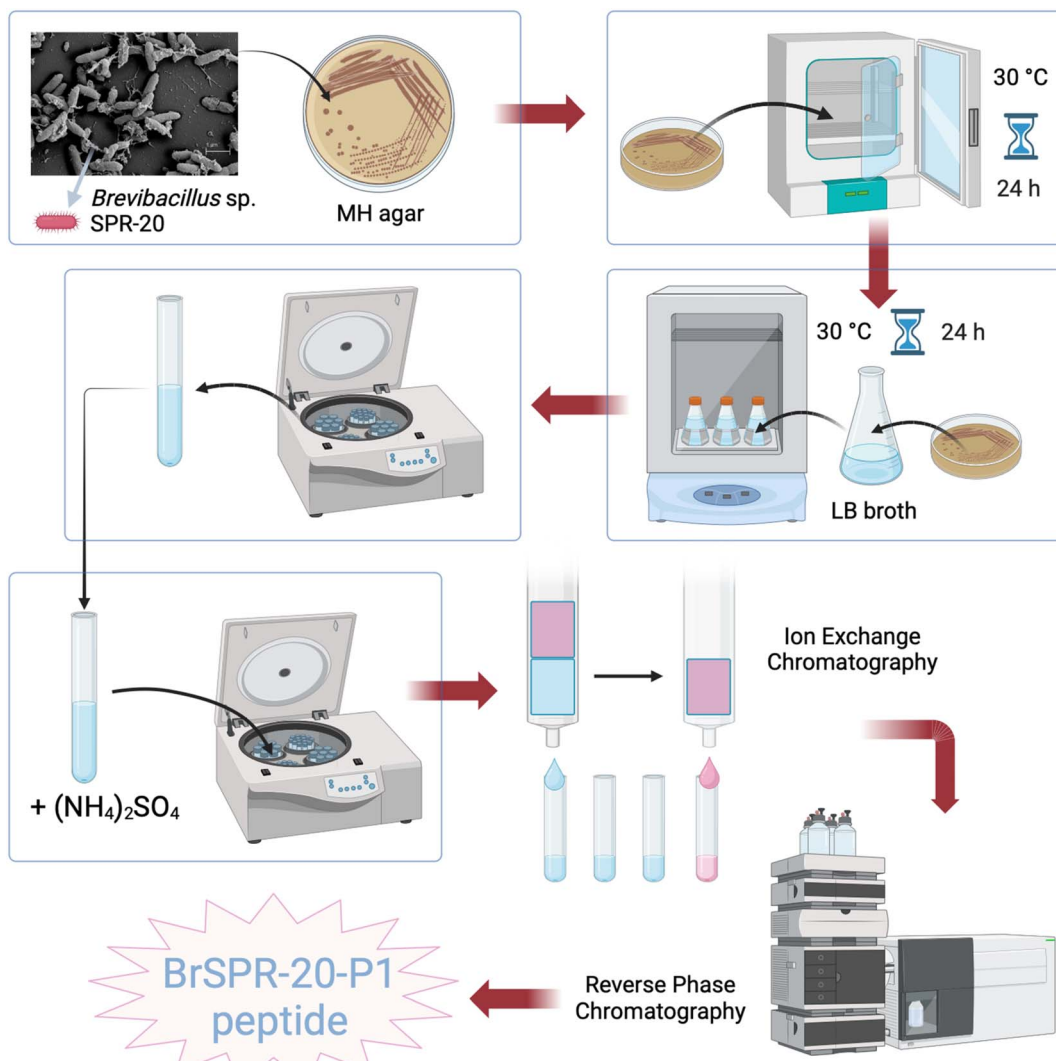


Fig. 2 Schematic diagram demonstrating the preparation of BrSPR-20-P1 antimicrobial peptide or P1-AMP-isolated and extraction from a *Brevibacillus* sp.

was washed 3 times with purified water to ensure that unentrapped P1-AMP was removed. The blank liposomes were prepared following the same method, without adding P1-AMP. The liposome dispersion was subjected to freeze-drying using

a 5% w/v of mannitol as a cryoprotectant. This process resulted in the formation of lyophilized liposome powder, which was then stored in an airtight container at 4 °C for further experiments.

Table 2 Composition of P1-AMP-loaded liposome formulations

Ingredients	Formulation codes/amount of ingredients (mg per batch)			
	F1	F2	F3	F4
P1-AMP	100	100	100	100
Cholesterol	50	50	50	300
l- $\alpha$ -Phosphatidylcholine (CH : PC weight ratio)	100 (1 : 2)	200 (1 : 4)	900 (1 : 18)	300 (6 : 6)
Chloroform <sup>a</sup>	10 mL	10 mL	10 mL	10 mL
Mannitol	500	500	500	500
Phosphate buffer saline pH 7.4 (10 mL) <sup>b</sup>	10 mL	10 mL	10 mL	10 mL
Theoretical solid content	750	850	1550	1200

<sup>a</sup> Chloroform undergoes evaporation while being prepared. It does not take weight into consideration. <sup>b</sup> The amount of buffering agent remaining after dialysis is negligible, and it is not included in the calculation of the total solid content weight.

## Preparation of P1-AMP-loaded liposome hydrogel

The P1-AMP-loaded liposome hydrogel was prepared by dispersing chitosan (0.5 g) in a mixture of acetic acid (0.2 mL), and glycerol (1.6 mL). The entrapment efficacy of formulation F3 was 39.39%; 40% was used for easy calculation. Therefore, the P1-AMP content in formulation F3 was 40 mg. Then, 745 mg of P1-AMP-loaded liposome freeze-dried powder, equivalent to P1-AMP 20 mg, was added to hydrogel, and the final weight was adjusted with purified water to 100 g. Therefore, the final concentration of P1-AMP in the hydrogel was 0.02% w/w. The obtained hydrogel was allowed to swell at room temperature for 48 h.

## Physicochemical characterization of P1-AMP- loaded liposome

**Particle size and zeta potential.** Before analysis, the lyophilized powder of P1-AMP-loaded liposome was reconstituted with distilled water in a ratio of 1 : 100. The ZetaSizer dynamic light-scattering analyzer (Malvern Panalytical Ltd., Malvern, UK) was used to measure the particle size, polydispersity index (PDI), and zeta potential.

**Surface morphology of liposome vesicles by scanning electron microscopy (SEM).** The size and morphology of P1-AMP-loaded liposomes were characterized by SEM (Carl Zeiss, Oberkochen, Germany). Prior to analysis, the lyophilized P1-AMP-loaded liposomes were placed on double-sided carbon adhesive tape uniformly coated with gold sputtering. Subsequently, the morphology of liposomes was examined at various magnification powers.

**Entrapment efficiency.** To determine the percentage of entrapment efficiency (%EE), the unentrapped P1-AMP was separated from the formulation using centrifugation. Briefly, the P1-AMP-loaded liposome dispersion was centrifuged at a speed of 18 000 rpm for 40 minutes (Sigma Centrifuge 4-16 KS, Osterode, Germany). Unentrapped P1-AMP was found in the supernatant, which was subsequently prepared and analyzed for P1-AMP content using Bradford protein assay according to the method described in the section on Protein determination by the Bradford protein assay. The total loading content of P1-AMP, which was used in the calculation, was 100 mg. The % EE was calculated following eqn (1):

$$\% \text{EE} = \frac{(\text{amount of total loading P1-AMP}) - (\text{amount of unentrapped P1-AMP})}{\text{amount of total loading P1-AMP}} \times 100 \quad (1)$$

## Physicochemical characterization of P1-AMP- loaded liposome hydrogel

**Appearance of hydrogel.** The appearance of the P1-AMP-loaded liposome hydrogel was examined by organoleptic observation, including color and transparency.

**pH.** The pH of P1-AMP-loaded liposome hydrogel was determined using a digital pH meter (Model 704, Metrohm, Herisau, Switzerland). Approximately 5 g of the hydrogel sample

was placed into a beaker. The pH values were measured after immersing the pH meter's probe into the hydrogel. The pH measurement was performed in triplicate, and the mean and standard deviation were reported.

**Rheogram and viscosity.** The viscosity of the P1-AMP-loaded liposome hydrogel was assessed using a Modular Advanced Rheometer System (HAAKE MARS 60; ThermoFisher Scientific, Bremen, Germany). The equipment was outfitted with a parallel plate design that had a diameter of 60 mm and a gap of 0.5 mm. Additionally, it had a Peltier temperature control system. The samples were placed onto the lower plate, and the upper plate was subsequently adjusted to fit the established gap. Flow studies were conducted within a range of shear rates from 1 to 10 000 s<sup>-1</sup> while maintaining a constant temperature of 25 °C.

## Fourier transform infrared spectroscopy (FT-IR)

Small amounts of all samples (~1 mg of each sample) including P1-AMP, P1-AMP-loaded liposome hydrogel, and blank liposome hydrogel were mixed into KBr pellets and compressed to obtain a 2 mm transparent disc with a hydraulic press before measurement of the IR spectra between 4000 and 400 cm<sup>-1</sup>, as determined by FT-IR spectroscopy (PerkinElmer, Inc., Waltham, MA, USA) at ambient temperature. All samples were freeze-dried before experimenting.

## Antimicrobial activity of P1-AMP-loaded liposome hydrogel

The minimum inhibitory concentration (MIC) of the purified P1-AMP, P1-AMP-loaded liposome hydrogel, blank liposome hydrogel, and blank hydrogel were determined by a broth microdilution assay following standard guidelines.<sup>20</sup> The P1-AMP-loaded liposome hydrogel was weighed and diluted with sterile water for injection to achieve a P1-AMP concentration ranging from 0.5 to 1024 µg mL<sup>-1</sup>. The purified P1-AMP was diluted by a cation-adjusted Mueller Hinton broth (CAMHB) to a concentration ranging from 0.5 to 1024 µg mL<sup>-1</sup>. The prepared samples were introduced into each well at a volume of 100 µL. Vancomycin (50 µg mL<sup>-1</sup>) and blank liposome hydrogel were used as positive and negative controls, respectively. CAMHB without tested bacteria was used as a blank.

*S. aureus* TISTR 517 and MRSA isolate 2468 were cultured in MH agar at 37 °C for 18 h. Single colonies of tested bacteria were dispersed in a CAMHB, and the turbidity was adjusted until the

absorbance at 625 nm was 0.1 to obtain 1 × 10<sup>8</sup> CFU mL<sup>-1</sup>. The bacterial suspension was further diluted to a concentration of 5 × 10<sup>6</sup> CFU mL<sup>-1</sup> with CAMHB. The diluted cell suspension (10 µL) was transferred to each well of a 96-well plate. The 96-well plates were incubated at 37 °C for 24 h, and the experiment was performed in triplicate for each strain. The MIC was evaluated by detecting the lowest concentration of the substances where no bacteria growth was observed. Afterward, 100 µL of each



dilution was spread evenly over MH agar and subsequently incubated at 37 °C for 24 h. The minimum bactericidal concentration (MBC) is regarded as the lowest concentration of the substances at which no colonies are observed.<sup>21</sup> All samples were tested in triplicate.

### Time kill assay

The *S. aureus* culture in CAMHB was standardized to an optical density of 0.1 at 625 nm. The cell suspension was diluted 1000 times before use. P1-AMP-loaded liposome hydrogel was prepared at concentrations of 1×, 5×, and 10× MIC in a medium and further diluted 20-fold by transferring 50 µL aliquots to 1000 µL. The final mixture was incubated for 0, 1, 2, 3, 6, 12, 18, and 24 h at 37 °C. The mixture incubated at each time point (10 µL) was 10-fold serially diluted with CAMHB. Additionally, MHA was plated with 10 µL of the serially diluted sample and incubated for 24 h at 37 °C. The number of bacterial colonies was quantified and expressed as CFU mL<sup>-1</sup>. Each test was performed in triplicate to ensure reliability.

### *In vitro* release of P1-AMP from P1-AMP-loaded liposome and P1-AMP-loaded liposome hydrogel

To study the *in vitro* release of P1-AMP from P1-AMP-loaded liposomes and P1-AMP-loaded liposome hydrogel, a modified Franz diffusion cell (MicroettePlus; Hanson Research, Chatsworth, CA, USA) was used according to a previous report.<sup>22,23</sup> The diffusion cell employed in this study was a glass tube with open ends, measuring 1.77 cm<sup>2</sup> in surface area. P1-AMP-loaded liposome hydrogel (1 g), P1-AMP-loaded liposomes (selected formulation F3), or P1-AMP alone were applied in the donor compartment. The medium (distilled water) in the receptor chamber was stirred continuously using a small magnetic bar. The 1 mL sample was collected from the receptor chamber at 0, 0.5, 1, 2, 4, 8, and 12 h. At each sampling point, an equal amount of distilled water was replenished to maintain the volume of the receptor phase. The samples were quantified for P1-AMP using a Bradford protein assay, as described in Protein determination section. The P1-AMP alone was used to determine drug release or dissolved as a control. Experiments were carried out in triplicate and performed at ambient temperatures (25–30 °C).

### *In vitro* permeability study

The transdermal permeation of P1-AMP-loaded liposome hydrogel was studied and compared with the transdermal permeation of P1-AMP-loaded liposomes and P1-AMP alone. The *in vitro* permeation was performed as described before using an automated Franz diffusion cell apparatus (MicroettePlus; Hanson Research, Chatsworth, CA, USA).<sup>24</sup> Strat-M® membranes (Millipore, Billerica, MA, USA) are synthetic, non-animal-based models that can substitute for human skin during transdermal diffusion testing and be mounted between the donor and receptor chambers of the Franz diffusion cells, with an effective diffusion area of 1.77 cm<sup>2</sup>. The receptor fluid consisted of a freshly prepared, 12 mL phosphate buffer solution (pH 7.4) maintained at 32 °C ± 0.5 °C. All samples equivalent to 200 µg of P1-AMP were applied to the donor

compartment through direct contact with the Strat-M® membranes. The diffusion cells were maintained in a shaking water bath (model 3047, Köttermann, Hänigsen, Germany) at 100 rpm, after which a 1 mL sample was collected at 0, 0.25, 0.5, 1, 2, 4, 6, 8, 10 and 12 h. At each sampling point, an equal amount of phosphate buffer pH 7.4 was replenished to maintain the volume of the receptor phase. The samples were quantified for P1-AMP using a Bradford protein assay, as described in the section concerning Bradford protein assay. All experiments were performed in triplicate. Transdermal flux ( $J$ ) (µg cm<sup>-2</sup> h<sup>-1</sup>) was calculated from the slope of the linear portion of drug permeated per cm<sup>2</sup> *versus* time. Permeability coefficient  $P_c$  (cm h<sup>-1</sup>) was calculated following eqn (2).

$$P_c = \frac{J}{C_d} \quad (2)$$

where  $C_d$  is the initial drug concentration in the donor compartment.

### Cytotoxicity assays

Human immortalized non-tumorigenic keratinocyte cell line (HaCaT) was used to examine the cytotoxicity of P1-AMP and P1-AMP-loaded liposome hydrogel. HaCaT (100 µL) was seeded in each well of a 96-well plate to obtain a density of 5000 cells per well in a complete media. Following 24 h of incubation, the culture media was replaced with 100 µL of purified P1-AMP (concentration 1.95–1000 µg mL<sup>-1</sup>) and P1-AMP liposomes loaded hydrogel, which had an equivalent P1-AMP concentration ranging from 1.56 to 200 µg mL<sup>-1</sup>. Before use, the hydrogel was diluted with sterile water for injection. PBS was employed as a negative control. Following a 24 h treatment of the cells, the sample was discarded and replaced with a fresh media containing 3-(4,5-dimethylthiazol-2-yl)-5-(3-carboxymethoxyphenyl)-2-(4-sulfophenyl)-2H-tetrazolium or MTS solution. The cells were incubated for 2 hours, and UV-vis absorbance was measured at a wavelength of 490 nm.

### *In vitro* wound healing by the scratch assay method

To evaluate the wound-healing activity of P1-AMP, the scratch wound healing test was employed to assess the migration process of fibroblast cells after stimulation with P1-AMP. The method employed in this research followed the approach outlined by Balekar *et al.* (2012).<sup>25</sup> In this study, L929 fibroblast cells were seeded at a density of  $5 \times 10^4$  cells per well of a 6-well plate. The cells were then incubated until a confluent monolayer was formed. A sterile pipette tip was used to generate a linear scratch on the monolayer. Cellular debris was removed and substituted with 2 mL of Dulbecco's Modified Eagle Medium (DMEM) containing a sample of P1-AMP 400 µg. The untreated group was used as a negative control. The images were observed under a microscope at a magnification of 10× and were captured at four time points: initial, 24, 48, and 72 h. The scratch closure distance of the images was evaluated quantitatively using computational software (ImageJ1.42q/Java1.6.0 10), and the percentage of cell migration rate was estimated. The mean of four independent replicates was calculated.



## Stability study

The P1-AMP-loaded liposome hydrogel (10 g) was placed in screw-cap amber glass vials to protect it from moisture and light. The samples were stored following the Association of Southeast Asian Nations Guidelines for testing the stability of pharmaceutical products in climatic zone IVb.<sup>26</sup> Samples were kept under accelerated settings of 40 °C and 75% relative humidity (RH), as well as long-term stability conditions of 30 °C and 75% RH. The formulations were assessed for their visual appearance, peptide concentration, pH level, and viscosity at intervals of 1, 3, and 6 months. P1-AMP dry powder (~200 µg) was loaded into a small polyethylene tube, and the stability condition was also performed according to this protocol to determine the appearance, assay, and antimicrobial activity as a control. Antibacterial activities were also reassessed at the conclusion of the 6 months research period.

## Results and discussion

### Antimicrobial activity of P1-AMP

A novel BrSPR-20-P1 antimicrobial peptide (P1-AMP) produced from *Brevibacillus* sp. SPR-20, the soil bacteria, was discovered by Songnaka *et al.* (2022). In their study, it was found that P1-AMP displayed potent antimicrobial activity against *S. aureus*, and MRSA.<sup>7</sup> The antimicrobial activity remained higher than 90% after being exposed to various conditions, such as high temperature (60–121 °C), proteolytic enzymes (proteinase K, trypsin, and  $\alpha$ -chymotrypsin), surfactants (sodium dodecyl sulfate and Triton X-100), and a wide pH range of 2–14.<sup>7</sup> However, the current study was conducted during a short period (15 min to 1 h). Notably, the stability of the peptide may be compromised if stored for an extended period or subjected to accelerated conditions. In our preliminary study, P1-AMP provided high antimicrobial activity against MRSA isolate 2468 with an inhibition zone of  $18.62 \pm 0.21$  mm (Fig. 3) at a concentration of  $118 \mu\text{g mL}^{-1}$ . Meanwhile, standard vancomycin provides a comparable result at a concentration of  $50 \mu\text{g mL}^{-1}$ . Therefore, P1-AMP exhibits the potential to function as a highly efficient antimicrobial peptide for the treatment of skin infections when considering its antimicrobial properties. In this study, the P1-AMP was assessed for its antimicrobial activity against *S. aureus* TISTR 517 and MRSA isolate 2468. The findings indicated that the MIC against TISTR 517 or MRSA isolate 2468 was  $2 \mu\text{g mL}^{-1}$ , whereas the MBC for both strains was  $4 \mu\text{g mL}^{-1}$  (see the results in Table 5). The obtained MIC and MBC agreed with the previous study of Songnaka *et al.* (2022).<sup>7</sup> As a result, this study developed a hydrogel formulation incorporating P1-AMP loaded liposomes with a final concentration of P1-AMP higher than 100 folds of MIC ( $200 \mu\text{g g}^{-1}$  of P1-AMP in hydrogel) for effective skin application in clinical studies.<sup>27,28</sup>

### Physicochemical properties of P1-AMP-loaded liposomes

Liposomes typically consist of PC as the primary lipid bilayer membrane component. Nevertheless, the ability of phospholipid hydrocarbon chains to rotate freely leads to the formation

of liposomes with leaky characteristics. The presence of CH restricts the rotation movement of the hydrocarbon chain. CH is inserted into the liposomal bilayer membrane, with its hydroxyl group towards the aqueous surface and its aliphatic chain aligned parallel to the acyl chain of phospholipid. This aids in the stabilization of the lipid bilayer membrane and reduces the leakage of hydrophilic substances that are enclosed within the membrane.<sup>29,30</sup> Therefore, this study aims to investigate the ideal ratio of PC and CH that can achieve maximum P1-AMP encapsulation while limiting leakage. Moreover, the small liposomes exhibit high efficacy in penetrating the cell membrane, whereas the zeta potential significantly influences the shelf stability of particle dispersions. The physicochemical properties of blank liposomes and P1-AMP-loaded liposomes are shown in Table 3. DLS is a technique employed to determine the mean hydrodynamic size and the degree of variation in the size distribution of submicron particles that are dispersed in a liquid. The PDI indicates the quality of the size distribution. Index values smaller than 0.05 are highly monodispersed, but PDI values larger than 0.7 indicate a broad particle size distribution.<sup>31</sup> The mean particle size of blank liposomes ranged from 324.5 to 1823.7 nm with a PDI ranging from 0.56 to 1.00, indicating liposome formulations were polydispersed. Considering formulations F1–F3, which contained equal CH but varied the amount of PC, it was shown that increasing the CH ratio to PC produced an increase in the liposome vesicles with a larger PDI. This is caused by the orientation of CH between PC molecules in the lipid bilayer membrane, resulting in the liposome being larger and more rigid.<sup>32,33</sup> However, both the concentration of CH and PC content in formulation F4 were

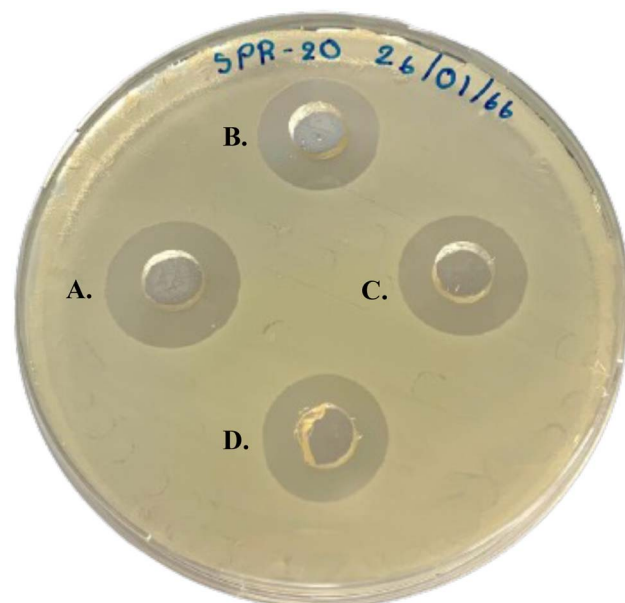


Fig. 3 Preliminary study of the antimicrobial activity of P1-AMP and standard vancomycin demonstrated a clear zone against MRSA isolate 2468 by the agar well diffusion method. The concentration of the standard vancomycin solution (A) was  $50 \mu\text{g mL}^{-1}$ , whereas the concentration of the P1-AMP solutions (B–D) was  $118 \mu\text{g mL}^{-1}$ .



increased as a result to achieve a final CH to PC ratio of 6 : 6. This resulted in the formation of a large and heterogeneous liposome vesicle with a PDI of 1.00, indicating an inappropriate liposome composition.

P1-AMP demonstrated hydrophilicity as a result of the amine and carboxylic group of amino acids. Therefore, P1-AMP should be trapped within the core of the hydrophilic liposome vesicle, generating a bigger particle size than an empty liposome.<sup>34,35</sup> The encapsulation effectiveness of liposomes is determined by the formulation's capacity to retain drug molecules, either in the aqueous core or in the bilayer membrane of the vesicles.<sup>35</sup> In the context of this investigation, an increase in lipid quantity and a decrease in CH ratio to PC resulted in a proportional improvement in the encapsulation efficacy of water-soluble substances like P1-AMP, as revealed in Table 3. Formulation F3, characterized by its high PC content of 900 mg, demonstrated the highest percentage of entrapment efficiency. Although formulation F4 had a larger PC concentration of 300 mg compared to formulations F1 and F2, it also had a higher ratio of CH to PC, which was 6 : 6. In addition, liposome vesicles obtained from formulation F4 appeared to be large and heterogeneous in size. This could be due to the presence of multilamellar vesicles (MLVs), which result in a smaller aqueous compartment between each membrane layer. As a consequence, the entrapment efficiency is lower. This is in accordance with the findings of Ullman, K. (2021), which observed that phospholipid concentration had a positive influence, whereas the addition of CH had an adverse impact on the efficiency of liposomal encapsulation.<sup>36</sup> This is because an increased lipid concentration produces a greater quantity of vesicles, thereby providing a larger internal volume for the encapsulation of the substance. Liposomes and membranes are generally stabilized by the addition of cholesterol. However, the bending modulus increases as CH levels increase. Consequently, membranes need more time to close after detachment from the interface, resulting in a greater loss of encapsulated substance. Therefore, finding the optimal CH:PC ratio is crucial for efficient encapsulation.

The zeta potential is commonly employed to assess the stability of colloidal dispersions. Colloidal dispersion systems with larger negative or positive zeta potential values are

electrically stable, while those with low zeta potential values tend to result in coagulation or flocculation.<sup>37</sup> A zeta potential value of a minimum  $\pm$  30 mV is considered to indicate stable liposomes.<sup>38–40</sup> In this study, the zeta potential of the blank liposome is in the range of  $-40.43$  to  $-60.17$  mV. However, the zeta potential changes from  $-57.33$  to  $-70.33$  mV when P1-AMP is added. The reduction in zeta potential of P1-AMP liposomes, as compared to blank liposomes, may be attributed to the dialysis process employed to remove the unentrapped P1-AMP. This dialysis process decreases the number of the bound ions or salts in the medium, thus affecting the charge of the liposome.<sup>41,42</sup> Nevertheless, the zeta potentials of all liposome formulations in this study were in the suitable range, which effectively prevented the formation of aggregation particles and ensured the stability of liposomal particles.<sup>38–40</sup>

To summarize, formulation F3, which contains PC : CH at a weight ratio of 18 : 1, provided the highest entrapment efficiency, small particle size, and suitable zeta potential values. These results were found to agree with the findings of previous reports on a high PC ratio with high entrapment efficacy.<sup>35</sup> Therefore, formulation F3 was chosen as a carrier for P1-AMP and incorporated into hydrogel formulation.

Based on the entrapment efficiency results, after the chosen liposome formulation (F3) was dialyzed to remove unentrapped P1-AMP, approximately 40% of P1-AMP remained entrapped in the liposome. The dialyzed liposome dispersion was then subjected to freeze-drying using mannitol as a cryoprotectant. As summarized in Table 2, the theoretical solid content of the liposome freeze-dry powder is 1490 mg, which consists of encapsulated P1-AMP (40 mg), cholesterol (50 mg), L- $\alpha$ -phosphatidylcholine (900 mg), and mannitol (500 mg). Nevertheless, the substances used in the preparation of the buffer are present in negligible amounts and can be cut off. As a result, 745 mg of freeze-dried liposome powder was equivalent to 20 mg of P1-AMP encapsulated in liposome vesicle.

SEM is used to study the topography and surface of materials such as liposome particles. Particle size and size distribution were also determined.<sup>43</sup> The morphology of liposomes (F3) was observed under SEM, as depicted in Fig. 4. Fig. 4A illustrates the spherical shape of the P1-AMP liposome vesicle before freeze-drying. The liposomes exhibited ovoid spheres with smooth

Table 3 Physical properties of blank liposome and P1-AMP-loaded liposomes (mean  $\pm$  SD,  $n = 3$ )

Formulation	F1	F2	F3	F4
CH : PC (weight ratio)	1 : 2	1 : 4	1 : 18	6 : 6
<b>Blank liposomes</b>				
Particle size (nm)	783.0 $\pm$ 9.0	330.3 $\pm$ 6.0	324.5 $\pm$ 8.6	1823.7 $\pm$ 288.2
Polydispersity index	0.82 $\pm$ 0.16	0.73 $\pm$ 0.07	0.56 $\pm$ 0.10	1.00 $\pm$ 0.00
Zeta potential (mV)	$-44.33 \pm 1.58$	$-40.43 \pm 2.51$	$-46.90 \pm 0.36$	$-60.17 \pm 0.93$
<b>P1-AMP-loaded liposomes</b>				
Particle size (nm)	1115.0 $\pm$ 110.7	435.6 $\pm$ 13.2	378.6 $\pm$ 14.0	2362.0 $\pm$ 255.6
Polydispersity index	0.88 $\pm$ 0.10	0.66 $\pm$ 0.10	0.66 $\pm$ 0.10	0.71 $\pm$ 0.25
Zeta potential (mV)	$-58.97 \pm 0.57$	$-57.33 \pm 0.72$	$-58.53 \pm 0.32$	$-70.33 \pm 0.15$
Entrapment efficiency (%)	27.22 $\pm$ 2.45	34.98 $\pm$ 1.03	39.39 $\pm$ 4.56	16.74 $\pm$ 5.20



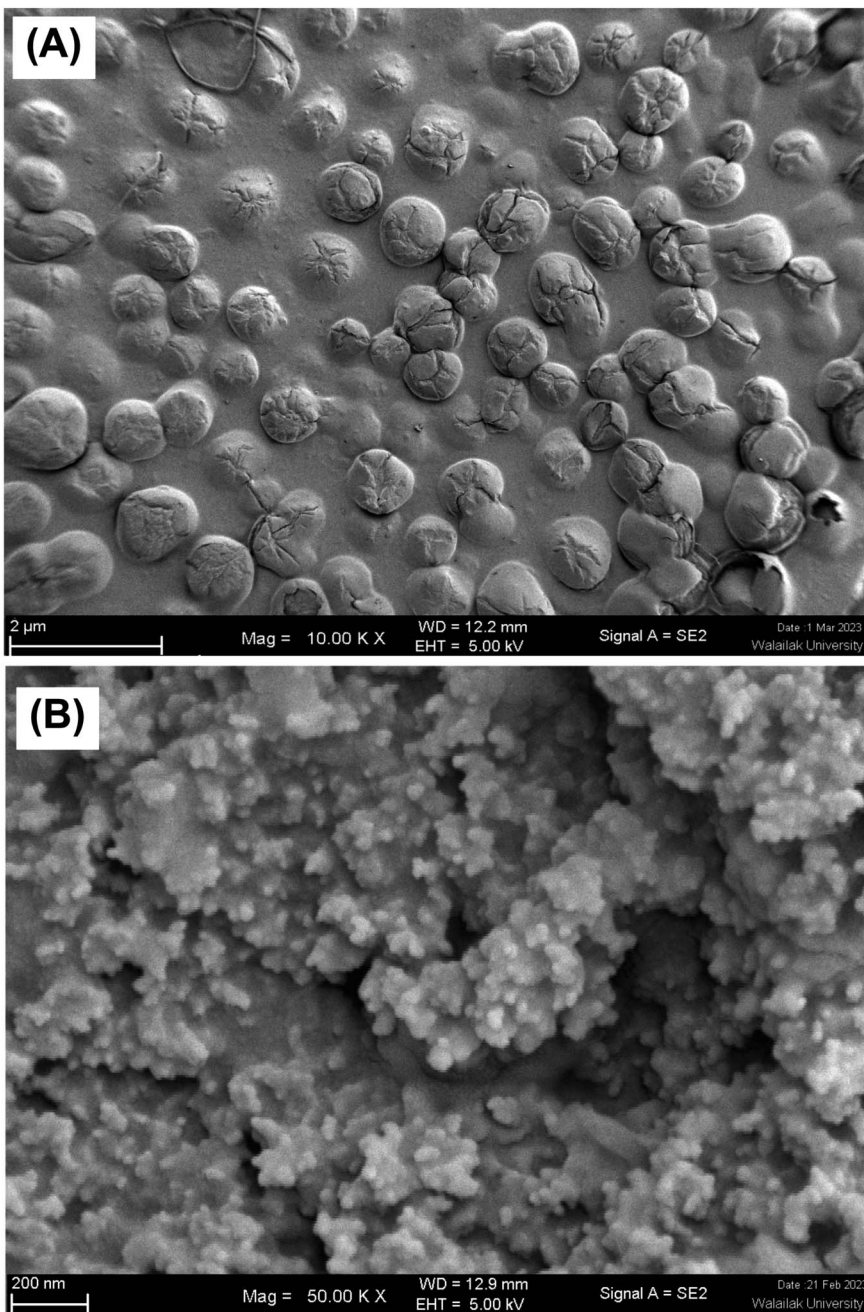


Fig. 4 Scanning electron microscope (SEM) images of selected liposomes (formulation F3). P1-AMP-loaded liposome dispersion before freeze-drying (A); freeze-dried powder of P1-AMP-loaded liposome (B).

surfaces. In contrast, the freeze-dried powder of P1-AMP-loaded liposomes (Fig. 4B) retained their spherical shape while having a smaller particle size compared to the size of liposome vesicles before freeze-drying. This reduction in size is attributed to the dehydration of liposomes.

#### Formulation development of P1-AMP-loaded liposome hydrogel

The topical hydrogel formulations were developed with a final concentration of P1-AMP, which was over 100 times greater than

the MIC against *S. aureus* TISTR 517 and MRSA isolate 2468 to ensure the effectiveness of the formulation when applied for clinical study.<sup>27,28</sup> Therefore, the hydrogel formulation was developed by incorporating 745 mg liposome freeze-dried powder that contained 20 mg of P1-AMP. This resulted in a final concentration of  $200 \mu\text{g g}^{-1}$  or 0.02% w/w of P1-AMP in a hydrogel.

The proposed structure of the developed P1-AMP liposome-loaded hydrogel is illustrated in Fig. 5. The P1-AMP peptides are water-soluble and thus should be encapsulated in the internal aqueous core of the liposome vesicle. When loading P1-



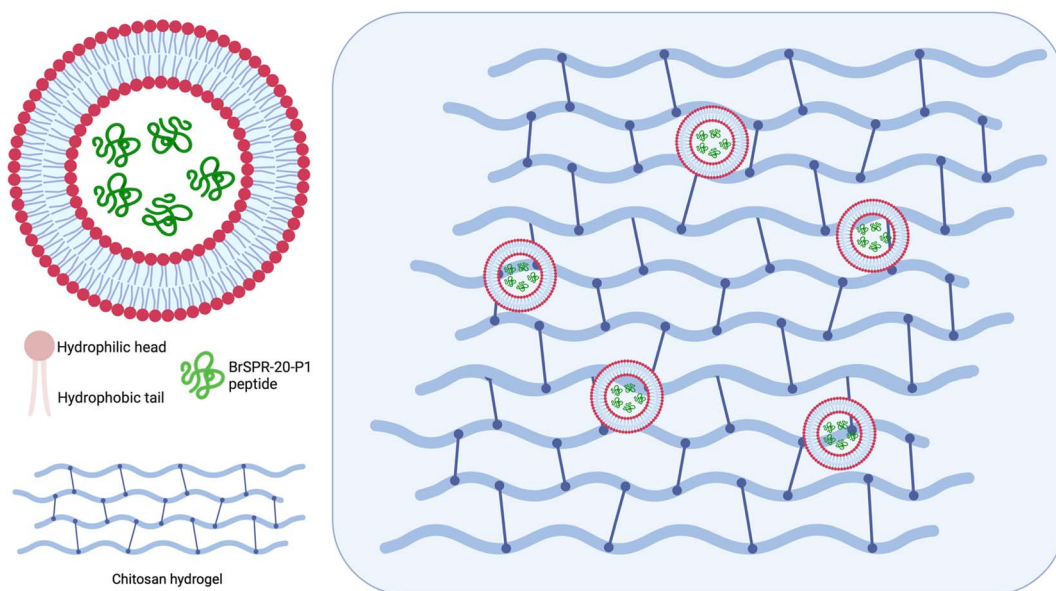


Fig. 5 Schematic diagram of the structure of P1-AMP liposomes prepared as a hydrogel.

AMP liposomes in the hydrogel, they were suspended thoroughly in the network structure of chitosan hydrogel.

Fig. 6A depicts the appearance of blank chitosan hydrogel. The formulation was found to be a yellowish, translucent, and very viscous gel with a pH of  $5.58 \pm 0.22$ . However, the resulting formulations were yellowish and viscous with a loss of translucent properties of chitosan hydrogel when P1-AMP-loaded liposome (F3) was incorporated (Fig. 6B). The pH of the P1-AMP-loaded liposome hydrogel was  $6.21 \pm 0.2$ , which was

significantly higher than blank chitosan hydrogel. The pH of normal undamaged skin falls within the acidic range of 4.5–5.0, which is considered optimal for maintaining skin health.<sup>44,45</sup> This acidity helps to regulate moisture levels, support the skin's protective barrier, prevent scaling, and promote the growth of beneficial microorganisms.<sup>44,45</sup> Optimal progress of normal acute wound healing has been observed to occur in a slightly acidic environment, which promotes fibroblast proliferation, epithelialization, angiogenesis, and microbial control when the

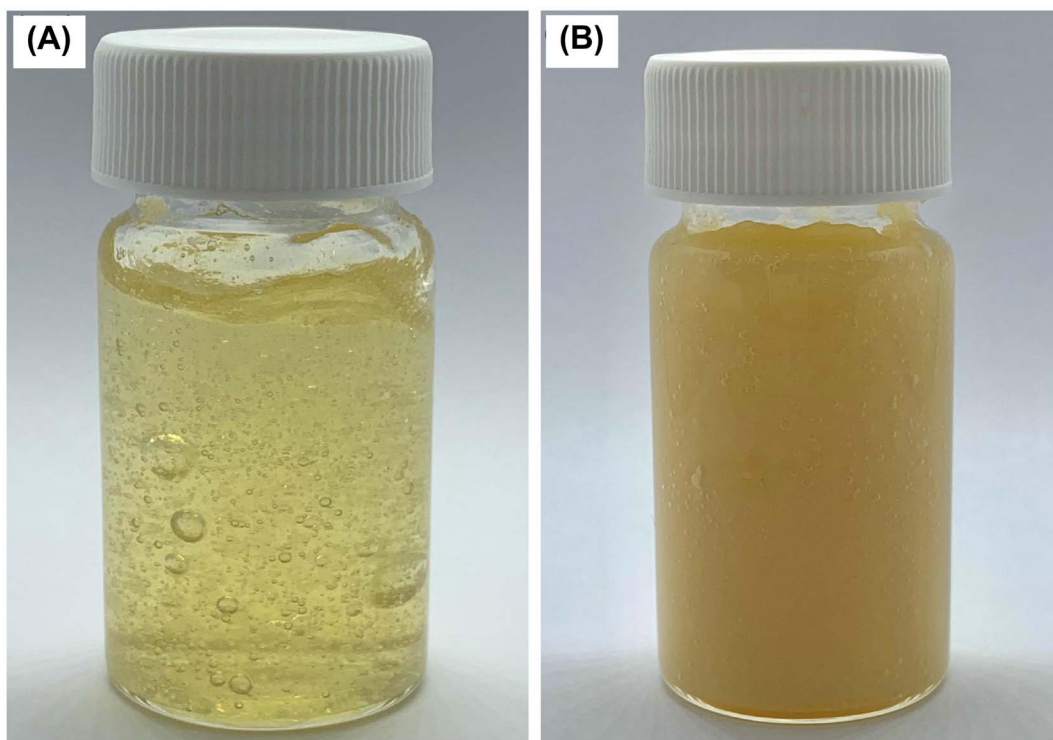


Fig. 6 Physical appearance of hydrogels showing (A) blank chitosan hydrogel, and (B) P1-AMP-loaded liposome hydrogel.



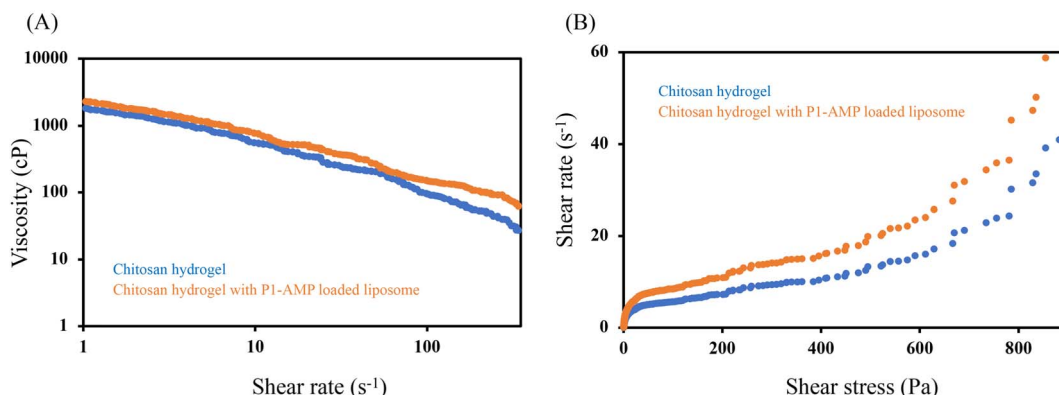


Fig. 7 Rheogram of blank chitosan hydrogel (blue curve) and P1-AMP-loaded liposome hydrogel (orange curve).

skin is breached. On the other hand, wounds that do not heal properly and instead worsen into long-lasting ailments are typically identified by having an alkaline pH level greater than 7.0.<sup>44</sup> However, the pH of P1-AMP-loaded liposome hydrogel had a weakly acidic pH and close to neutral pH. Therefore, it does not cause skin irritation and is suitable for acidic wound skin, which is common in the early stages of infected wounds.<sup>46</sup>

Viscosity determination is an important physical property used to determine the resistance of flow materials. It is defined as shear stress divided by shear rate. If the product has a suitable viscosity value, it will be easy to apply and spread on the skin. The viscosity of P1-AMP liposome-loaded hydrogel was  $758.0 \pm 149.8$  cP compared to blank chitosan hydrogel, which was  $683.1 \pm 66.5$  cP determined at a shear rate of  $10 s^{-1}$  (Fig. 7A). The rheogram showed pseudoplastic behavior with a shear thinning system (Fig. 7B).

The FT-IR results of P1-AMP, blank liposome hydrogel and P1-AMP-loaded liposome hydrogel formulation F3 are shown in Fig. 8. The main structure of P1-AMP consisted of  $-\text{NH}_2$  and  $-\text{COOH}$ , which was an amino acid structure. The broad-spectrum

peak shown at  $3355.45\text{ cm}^{-1}$  indicated  $-\text{NH}_2$  stretching with a sharp peak at  $1555.18\text{ cm}^{-1}$  indicated  $-\text{NH}_2$  bending. The  $-\text{COOH}$  also overlapped at  $-\text{NH}_2$  stretching ( $3355.45\text{ cm}^{-1}$ ). The ester group ( $-\text{CO}-\text{NH}_2$ ) showed a spectrum peak at  $1649.31\text{ cm}^{-1}$  that was found in the amino acid Asn. In addition, the methyl group ( $-\text{CH}_3$ ) found in Val and Leu showed bending spectrum peaks at  $1408.53\text{ cm}^{-1}$  and  $1343.29\text{ cm}^{-1}$ .<sup>47</sup>

The blank liposome hydrogel (freeze-dried) showed IR peaks at  $3392.30\text{ cm}^{-1}$  and  $1463.96\text{ cm}^{-1}$  ( $-\text{NH}_2$ ). The peak at the wavenumber  $2929.69$  was  $-\text{OH}$  with hydrogen bonded. The P1-AMP-loaded liposome hydrogel (freeze-dried) consisted of CH, PC, mannitol, and chitosan. The FT-IR spectrum showed a peak at  $3283.77\text{ cm}^{-1}$  that corresponded with  $-\text{OH}$  (H-bonded). The spectrum peaks at  $3390.73$  and  $1562.39\text{ cm}^{-1}$  corresponded with  $-\text{NH}_2$  stretching and  $-\text{NH}_2$  bending, respectively. The carboxylic group showed a peak at  $2918.44\text{ cm}^{-1}$ . The functional group  $-\text{C}-\text{O}-\text{C}-$  was found to peak at  $1300-1000\text{ cm}^{-1}$ . The methyl group was also found at  $1411.36\text{ cm}^{-3}$ .<sup>47</sup> The wave number of characteristic peaks in the P1-AMP FT-IR spectrum

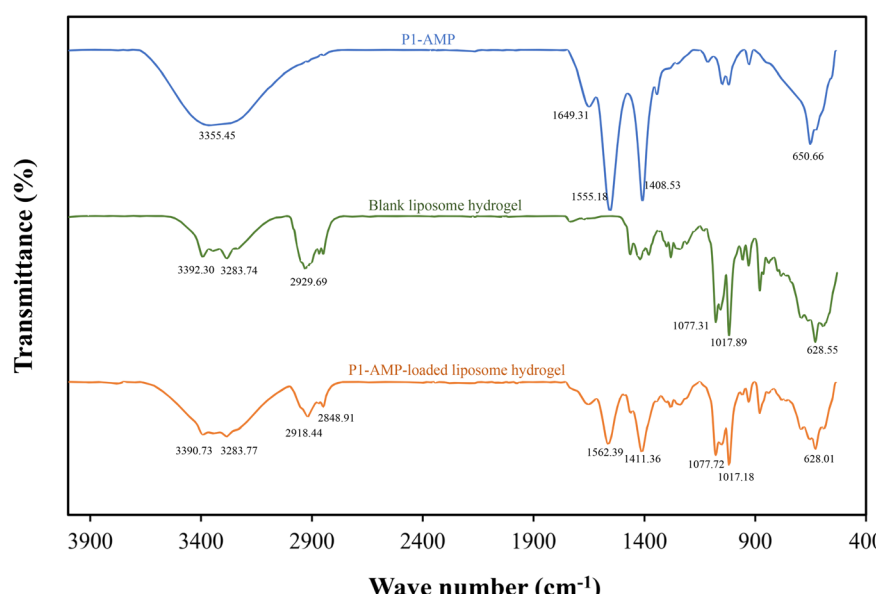
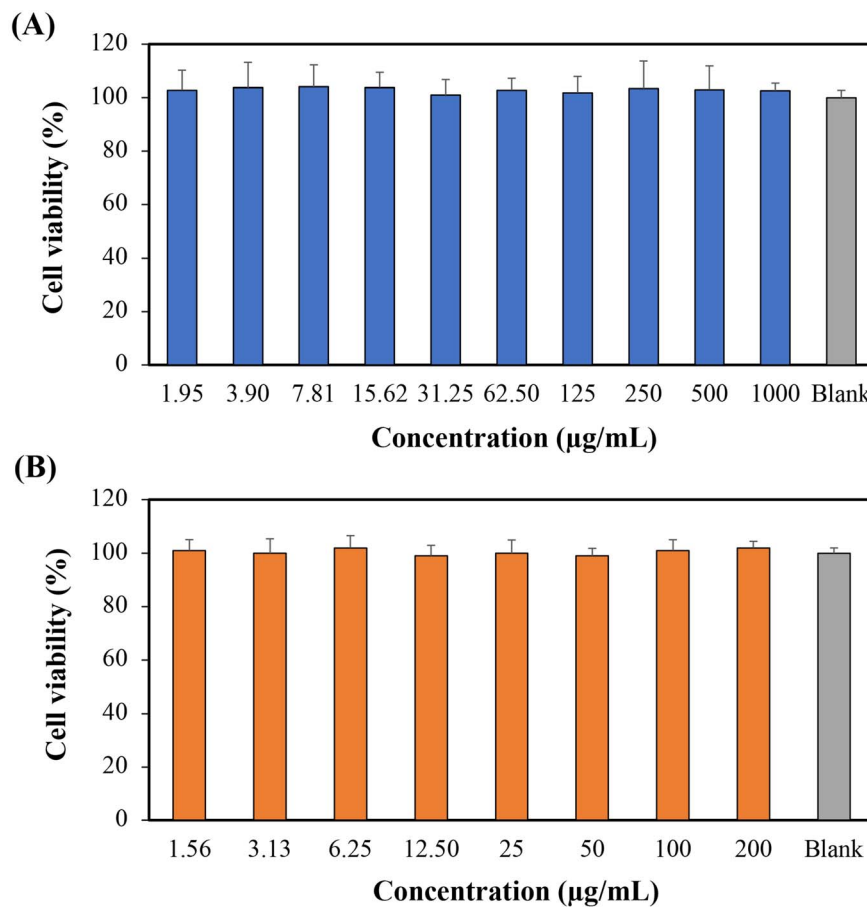


Fig. 8 FT-IR spectrum of P1-AMP (blue line), blank liposome hydrogel without peptide (green line), and P1-AMP-loaded liposome hydrogel (formulation F3) (orange line).





**Fig. 9** Cell viability of human keratinocyte epithelial cells. The cells were treated with P1-AMP at a concentration of  $1.95\text{--}1000\text{ }\mu\text{g mL}^{-1}$  (A), and with P1-AMP-loaded liposome hydrogel at a concentration equivalent to P1-AMP of  $1.56\text{--}200\text{ }\mu\text{g mL}^{-1}$  (B). The symbol \* indicates the significant difference in % cell viability when compared to the blank ( $p\text{-value} < 0.05$ ).

shifted, indicating the interaction when formulated as P1-AMP-loaded liposome hydrogel.

#### *In vitro* cytotoxicity of P1-AMP-loaded liposome hydrogel

Cell viability following exposure to P1-AMP and P1-AMP-loaded liposome hydrogel is shown in Fig. 9(A) and (B). When the HaCaT cell was treated with P1-AMP at a concentration ranging from  $1.95$  to  $1000\text{ }\mu\text{g mL}^{-1}$ , it revealed cell viability of  $100\%$ . This indicated that P1-AMP did not induce adverse effects within the measured concentration range. The P1-AMP-loaded liposome hydrogel, with a concentration equivalent to P1-AMP ranging from  $1.56$  to  $200\text{ }\mu\text{g mL}^{-1}$ , demonstrated a cell viability of  $100\%$ . This suggested that P1-AMP did not cause any toxicity to the keratinocyte epithelial cells within  $24\text{ h}$  of exposure. The results indicated that the use of this hydrogel for treating infected skin or wounds does not appear to raise concerns about its biocompatibility. Nevertheless, *in vivo* studies should be performed before clinical application.

#### Wound healing activities of P1-AMP

The ability of P1-AMP to promote cell migration and accelerate wound healing was examined in comparison to the negative untreated control. The P1-AMP was employed at a concentration

of  $200\text{ }\mu\text{g mL}^{-1}$ , which is the equivalent concentration in the hydrogel formulation. This concentration did not cause toxicity to the L929 fibroblast cells that was previously examined (data not shown). The wound was observed under an inverted light microscope after being treated with P1-AMP for  $24$ ,  $48$ , and  $72$  hours, and the percentage of migration at each time point was estimated relative to the initial observation. The results of this observation are shown in Fig. 10(A) and (B). P1-AMP exhibited a significantly greater percentage of cell migration after  $24$  and  $48$  hours of exposure ( $p\text{-value} < 0.05$ ). The results showed that applying P1-AMP resulted in the accelerated healing of wounds compared to the untreated control.

#### *In vitro* release profiles and permeability of P1-AMP

The release behavior of P1-AMP from P1-AMP-loaded liposome hydrogel at  $37\text{ }^\circ\text{C}$  is presented in Fig. 11A. The results showed that the P1-AMP content released from both liposome and liposome-loaded hydrogel reached  $80\%$  within  $12\text{ h}$ . P1-AMP was rapidly dissolved  $>90\%$  in  $1\text{ h}$ , indicating that the solubility of P1-AMP had no effect on drug release. P1-AMP rapidly released from liposomes because of the high gradient concentration of peptide and the hydration of liposomes, whereas the slow release of the P1-AMP was observed after  $4\text{ h}$ . The release



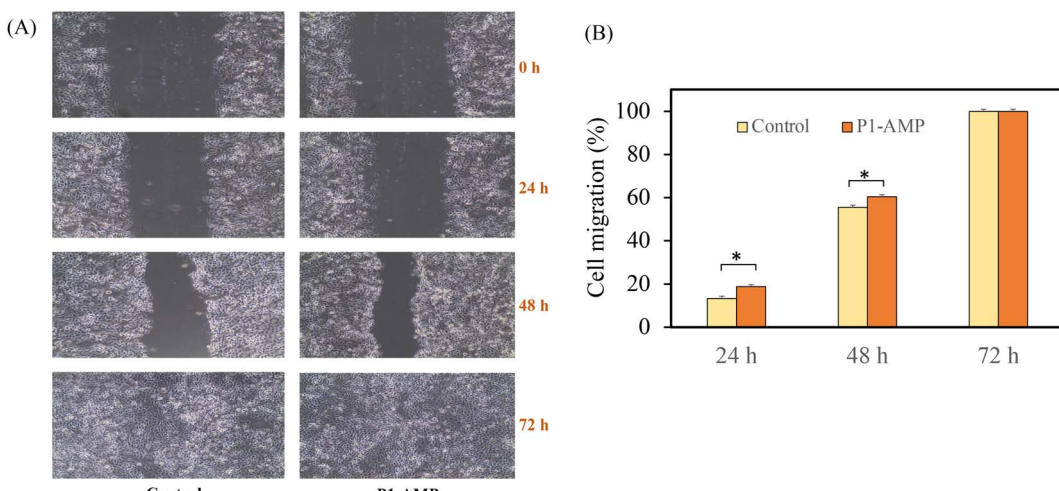


**Fig. 10** Measurement of cell migration in the *in vitro* scratch assay. A fibroblast cell lines (L929) layer subjected to scratch and treated with P1-AMP 200  $\mu\text{g mL}^{-1}$  at initial, 24 h, 48 h, and 72 h after incubation observed under an inverted light microscope (A). The percentage of cell migration (B). Asterisk (\*) indicates the significant differences ( $p$ -value  $< 0.05$ ) compared to treated and non-treated control samples at the same intervals.

profile of P1-AMP from liposome and liposome-loaded hydrogel was in a similar trend, in which P1-AMP was released faster from liposomes than liposome-loaded hydrogel by about 5–10%. This is caused by the matrix of polymer composed in hydrogel formulation creating viscosity, and thus retarding P1-AMP release. A chitosan hydrogel system could control the release of hydrophilic and peptide substances within hours or

in several days depending on various parameters such as formulation, preparation method (*chemical* or *physical*, *in situ* gelation), pH, and temperature.<sup>48</sup>

Fig. 11B displays the permeability of P1-AMP-loaded liposomes and P1-AMP-loaded liposome hydrogel compared to P1-AMP alone. This study found that the permeability was linear during the first 6 h, but the permeability value was relatively constant after the 6 h period. The maximum drug permeability is approximately 80%. However, P1-AMP alone cannot penetrate the membrane at all times, probably due to the polarity of the peptide, which makes it unable to pass through.<sup>49</sup> The Flux ( $J$ ) value of the P1-AMP-loaded liposome was  $12.9 \pm 4.1 \text{ mg cm}^{-2} \text{ h}^{-1}$ , which is about 22% more than the value of the P1-AMP-loaded liposome hydrogel, which was  $10.6 \pm 1.2 \text{ mg cm}^{-2} \text{ h}^{-1}$  (Table 4). The hydrophilic and polymer properties of chitosan hydrogel led to a slower release of P1-AMP in the liposome system.<sup>50</sup> During the first 2 h, P1-AMP was dissolved almost completely, but in the liposome or liposome hydrogel system, it was only 60–70% (Fig. 11A). This is in line with the results of the membrane permeability, which was 25–40% during the first 2 h. As a result, the dissolution or release of P1-AMP does not act as a permeability barrier. The permeation enhancer used in the formulation is another effective option. It can be used to increase the permeability through the Strat-M® membrane of hydrophilic nature and the high molecular weight of this innovative peptide.<sup>51</sup> However, it may not necessarily increase penetration into the skin if considering the use of a P1-AMP-loaded liposome hydrogel in a topical dosage form. The ability of the drug to penetrate the upper layer of the skin and act as an antimicrobial agent in the infected skin area may be sufficient for its application.

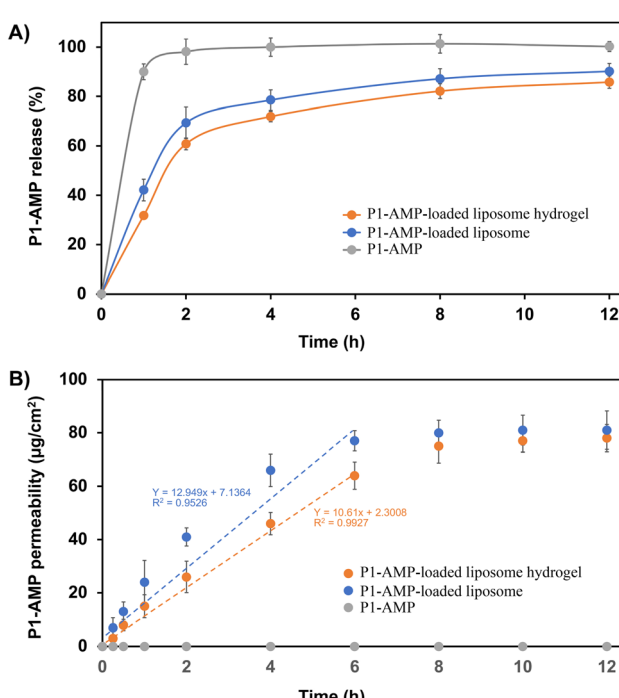


**Fig. 11** Percentage of P1-AMP releases from liposome and P1-AMP-loaded liposome hydrogel compared to P1 AMP alone (A). P1-AMP permeability from liposome and P1-AMP-loaded liposome hydrogel compared to P1-AMP alone (B). Results are expressed as percentage mean  $\pm$  SD.

### Antimicrobial activity of P1-AMP-loaded liposome hydrogel

In this investigation, the antibacterial activity of P1-AMP, P1-AMP-loaded liposome hydrogel, blank liposome hydrogel, and blank hydrogel against *S. aureus* TISTR 517 and MRSA isolate 2468 was



**Table 4** P1-AMP *in vitro* permeability through Strat-M membrane after 6 h (mean  $\pm$  SD,  $n = 3$ )

Formulation	Flux ( $J$ ) ( $\mu\text{g cm}^{-2} \text{h}^{-1}$ )	Permeability coefficient ( $P_c$ ) ( $\text{cm h}^{-1}$ )
P1-AMP	$0 \pm 0.00$	$0 \pm 0.0$
P1-AMP-loaded liposome	$12.9 \pm 4.1$	$3.2 \times 10^{-3}$
P1-AMP-loaded liposome hydrogel	$10.6 \pm 1.2$	$2.6 \times 10^{-3}$

investigated. The purpose was to evaluate the synergistic effect of the formulation. As presented in Table 5, blank liposome hydrogel and blank hydrogel did not exert antimicrobial activity against either tested strain, whereas P1-AMP and P1-AMP-loaded liposome hydrogel gave the same MIC and MBC against *S. aureus* TISTR 517 and MRSA isolate 2468 of 2 and  $4 \mu\text{g mL}^{-1}$ , respectively. The obtained MIC and MBC of P1-AMP agreed with a previous study.<sup>7</sup> Currently, several reported AMPs have been revealed to be excellent drug candidates for clinical exploitation due to their numerous advantages, including biocompatibility, biodegradability, and ease of synthesis and modification.<sup>52</sup> In this study, P1-AMP exhibited equivalent antibacterial effectiveness to Vancomycin, although it was formulated as a gel.

The time-kill kinetics of P1-AMP-loaded liposome hydrogel against *S. aureus* TISTR 517 are illustrated in Fig. 12. Significant reductions in bacterial growth were observed at all tested concentrations ( $1\times$ ,  $5\times$ , and  $10\times$  MIC) with as little as 1 hour of incubation. The most pronounced decrease in cell numbers occurred between 4 and 6 hours across all concentrations, corresponding with the burst release of P1-AMP from the liposome hydrogel within the first 4 hours. Eradication effects were observed at 6, 12, and 24 hours for  $10\times$ ,  $5\times$ , and  $1\times$  MIC, respectively, indicating a concentration-dependent response. The previous research established that the killing effect of P1-AMP is directly proportional to both its concentration and the duration of exposure.<sup>7</sup>

### Stability of P1-AMP-loaded liposome hydrogel

The stability of P1-AMP, both in its free form and when encapsulated within a liposome hydrogel, was evaluated following storage under controlled conditions at  $30^\circ\text{C}$  and 75% RH, and under accelerated conditions at  $40^\circ\text{C}$  and 75% RH for periods of 3 and 6 months. The results are presented in Table 6. As a control, the P1-AMP stored in a polyethylene tube at  $30^\circ\text{C}$  and 75% RH for 3 months demonstrated a decrease in peptide content to 67%.

**Table 5** MIC and MBC of P1-AMP liposome-loaded hydrogel formulation and control

Formulation	MIC/MBC <i>S. aureus</i> TISTR 517 ( $\mu\text{g mL}^{-1}$ )	MIC/MBC MRSA isolate 2468 ( $\mu\text{g mL}^{-1}$ )
P1-AMP liposome-loaded hydrogel (equivalent amount of P1-AMP)	2/4	2/4
Blank liposome-loaded hydrogel	— <sup>a</sup>	— <sup>a</sup>
Blank hydrogel (chitosan)	— <sup>a</sup>	— <sup>a</sup>
P1-AMP	2/4	2/4
Vancomycin	2/2	2/2

<sup>a</sup> No inhibition at a concentration of  $0.5\text{--}1024 \mu\text{g mL}^{-1}$ .

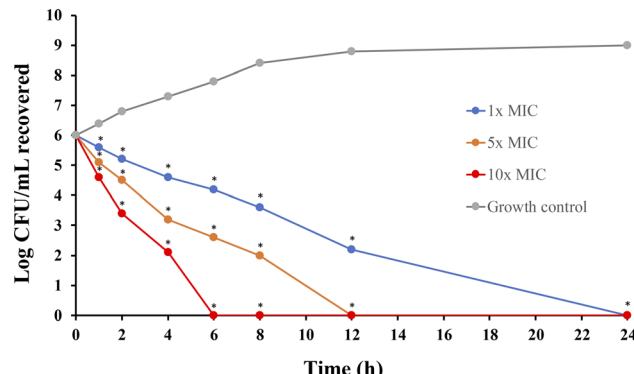


**Fig. 12** Time-kill kinetics curve of P1-AMP-loaded liposome hydrogel against *S. aureus* TISTR 517 at concentrations of  $1\times$ ,  $5\times$ , and  $10\times$  MIC values. An asterisk (\*) indicates a significant difference ( $p$ -value  $< 0.05$ ) compared to treated and non-treated samples at the same intervals.

When subjected to the accelerated storage conditions of  $40^\circ\text{C}$  and 75% RH, the peptide content further declined to 40%. These results indicate that both temperature and humidity significantly affect the stability of P1-AMP. In contrast, the P1-AMP-loaded liposome hydrogel exhibited remarkable physical stability, showing no significant changes in key characteristics such as appearance, pH, and viscosity. Throughout all testing conditions and durations, the assay revealed that the P1-AMP content in the liposomal formulation remained between 90.0% and 100.0% of the theoretical content, corresponding to 0.02% w/w of P1-AMP. However, the stability assessment indicated a more pronounced reduction in P1-AMP levels at  $40^\circ\text{C}$  compared to  $30^\circ\text{C}$ , potentially due to thermal effects on the peptide. Regarding antimicrobial activity, the MIC of the P1-AMP-loaded liposome hydrogel remained stable at  $2 \mu\text{g g}^{-1}$ , despite a decrease in peptide content from 98% to 91% of the initial concentration. This finding aligns with the observed reduction in bactericidal activity, which can be attributed to hydrolysis of P1-AMP during storage at both  $30^\circ\text{C}/75\%$  RH and  $40^\circ\text{C}/75\%$  RH. The enhanced stability of P1-AMP within liposomes can be attributed to several mechanisms.<sup>53</sup> Notably, liposomes protect the encapsulated P1-AMP from adverse environmental factors such as oxygen, light, and moisture, which are known to contribute to the degradation of sensitive molecules like peptides and proteins. Additionally, certain liposomal formulations may promote the stability of drug molecules by forming stable complexes, thereby preventing destabilization or inactivation.<sup>54</sup> These attributes make liposomes a promising strategy in drug delivery, particularly for biologics and other pharmaceuticals that are inherently unstable.



**Table 6** Stability of P1-AMP and P1-AMP-loaded liposome hydrogel after storage at 30 °C and 75% RH and in accelerated conditions at 40 °C and 75% RH for 3, 6 months. Data are represented in mean ± standard deviation ( $n = 3$ )

Test	Initial	Storage conditions			
		30 °C ± 2 °C/75 ± 5% RH	40 °C ± 2 °C/75 ± 5% RH	3 months	6 months
<b>P1-AMP</b>					
Appearance	Off-white to pale yellow powder	Off-white to pale yellow powder	NA <sup>c</sup>	Off-white to pale yellow powder	NA <sup>c</sup>
Assay	99.92 ± 0.22	67.34 ± 0.45	NA <sup>c</sup>	40.45 ± 4.28	NA <sup>c</sup>
MIC against <i>S. aureus</i> (μg mL <sup>-1</sup> )	2	16	NA <sup>c</sup>	128	NA <sup>c</sup>
<b>P1-AMP-loaded liposome hydrogel</b>					
Appearance	Yellow hydrogel	Yellow hydrogel	Yellow hydrogel	Yellow hydrogel	Yellow hydrogel
P1-AMP content (%LA) <sup>a,b</sup>	98.20 ± 0.20	95.50 ± 0.12	92.32 ± 1.21	92.35 ± 0.73	91.34 ± 1.15
pH	6.21 ± 0.20	6.10 ± 0.00	6.12 ± 0.10	6.22 ± 0.10	6.08 ± 0.00
Viscosity (cP)	758.0 ± 149.8	784.5 ± 102.2	759.1 ± 79.1	722.2 ± 131.0	712.4 ± 89.5
MIC against <i>S. aureus</i> (μg mL <sup>-1</sup> )	2	NA <sup>c</sup>	2	NA <sup>c</sup>	2

<sup>a</sup> %LA = % labeled claim. <sup>b</sup> Theoretical content of P1-AMP in the hydrogel is 0.02% w/w. <sup>c</sup> NA = not applicable.

## Conclusion

P1-AMP is a novel peptide isolated from *Brevibacillus* sp. SPR-20. It exhibits strong antimicrobial activity and wound-healing activity. This study developed and investigated the efficacy of P1-AMP-loaded liposome hydrogel as a topical anti- *S. aureus* and anti-MRSA formulation. The selected P1-AMP-loaded liposome (formulation F3), composed of PC:CH in a ratio of 18:1, demonstrated the highest encapsulation efficiency with a suitable particle size and zeta potential. P1-AMP-loaded liposome has a spherical shape with negative charges and significantly enhances the permeability of P1-AMP through the skin compared to P1-AMP without encapsulation in the liposome. After developing the P1-AMP-loaded liposome formulation (F3) as topical hydrogel, the P1-AMP was rapidly released from the liposome hydrogel within an initial 8 h. The formulation exhibited good antimicrobial activity, comparable to that of standard vancomycin, and did not induce cytotoxicity to tested keratinocyte cells. The liposome significantly increased the stability of P1-AMP when stored at 30 °C and 40 °C with high humidity for at least 6 months under the studied conditions. However, further study of the developed P1-AMP-loaded liposome hydrogel is required to determine its efficacy in animal models or clinical testing in infected skin before commercial application.

## Abbreviations

AMP	Antimicrobial peptide
BrSPR-20-P1 (P1-AMP)	Novel peptide isolated from <i>Brevibacillus</i> sp. The structure is NH <sub>2</sub> -VVVNVLVKVLPPPVV-COOH
BSA	Bovine serum albumin

CAMHB	Cation-adjusted Mueller Hinton broth
CFU	Colony forming unit
CH	Cholesterol
DMEM	Dulbecco's Modified Eagle Medium
FT-IR	Fourier transform infrared spectroscopy
H	Hydrophobicity
HaCaT	Human immortalized non-tumorigenic keratinocyte cell line
LB	Luria-Bertani
MBC	Minimum bactericidal concentration
MH	Mueller Hinton
MIC	Minimum inhibitory concentration
MLVs	Multilamellar vesicles
MRSA	Methicillin-resistant <i>Staphylococcus aureus</i>
MTS	3-(4,5-Dimethylthiazol-2-yl)-5-(3-carboxymethoxyphenyl)-2-(4-sulfophenyl)-2H-tetrazolium
OD	Optical density
PBS	Phosphate-buffered saline
PC	L- $\alpha$ -Phosphatidylcholine
PDI	Polydispersity index
pI	Isoelectric point
RH	Relative humidity
rpm	Revolutions per minute
SEM	Scanning electron microscopy
TISTR	Thailand Institute of Scientific and Technological Research
UV-vis	Ultraviolet-visible

## Data availability

Data are available upon request from the authors.



## Author contributions

Narumon Changsan: data curation, formal analysis, investigation, methodology, validation, visualization, writing—original draft, writing – review & editing. Apichart Atipairin: conceptualization, data curation, formal analysis, funding acquisition, investigation, methodology, validation, visualization, writing – original draft, writing – review & editing. Pajaree Sakdiset: data curation, formal analysis, investigation, methodology, validation, visualization, writing—original draft, writing – review & editing. Poowadon Muenraya: data curation, formal analysis, investigation, methodology, validation, visualization, writing—original draft, writing – review & editing. Rutthapol Sritharadol: investigation, methodology, validation, visualization, writing—original draft, writing – review & editing. Teerapol Srichana: conceptualization, data curation, formal analysis, funding acquisition, investigation, methodology, validation, visualization, writing—original draft, writing – review & editing. Neelam Balekar: formal analysis, writing – original draft, writing – review & editing. Suranate Phanapithakkun: formal analysis, investigation, writing – review & editing. Somchai Sawatdee: conceptualization, data curation, formal analysis, funding acquisition, investigation, methodology, project administration, supervision, validation, visualization, writing—original draft, writing – review & editing.

## Conflicts of interest

The authors declare that they have no conflict of interest.

## Acknowledgements

This work was partially supported by The Center for Scientific and Technological Equipment and School of Pharmacy Walailak University through the course of PHD-571 Special Projects in Pharmacy and research grant from Drug and Cosmetics Excellence center, Walailak University, Thailand. We would like to thank the scientist in the Drug Delivery System Excellence Center, Faculty of Pharmaceutical Sciences, Prince of Songkla University for laboratory assistant.

## References

- 1 A. Moretta, C. Scieuzzo, A. M. Petrone, R. Salvia, M. D. Manniello, A. Franco, D. Lucchetti, A. Vassallo, H. Vogel, A. Sgambato and P. Falabella, Antimicrobial peptides: a new hope in biomedical and pharmaceutical fields, *Front. Cell. Infect. Microbiol.*, 2021, **11**, 668632, DOI: [10.3389/fcimb.2021.668632](https://doi.org/10.3389/fcimb.2021.668632).
- 2 A. Penesyan, M. Gillings and I. T. Paulsen, Antibiotic discovery: combatting bacterial resistance in cells and biofilm communities, *Molecules*, 2015, **20**, 5286–5298, DOI: [10.3390/molecules20045286](https://doi.org/10.3390/molecules20045286).
- 3 A. Herman and A. P. Herman, Antimicrobial peptides activity in the skin, *Skin Res. Technol.*, 2019, **25**, 111–117, DOI: [10.1111/srt.12626](https://doi.org/10.1111/srt.12626).
- 4 S. Gera, E. Kankuri and K. Kogerman, Antimicrobial peptides – unleashing their therapeutic potential using nanotechnology, *Pharmacol. Ther.*, 2022, **232**, 107990, DOI: [10.1016/j.pharmthera.2021.107990](https://doi.org/10.1016/j.pharmthera.2021.107990).
- 5 Q. Zhang, Z. Yan, Y. Memg, X. Hong, G. Shao, J. Ma, X. Cheng, J. Liu, J. Kang and C. Fu, Antimicrobial peptides: mechanism of action, activity and clinical potential, *Military Med. Res.*, 2021, **8**, 48, DOI: [10.1186/s40779-021-00343-2](https://doi.org/10.1186/s40779-021-00343-2).
- 6 N. Songnaka, M. Lertcanawanichakul and A. Atipairin, Promising anti-MRSA activity of *Brevibacillus* sp. isolated from soil and strain improvement by UV mutagenesis, *Sci. Pharm.*, 2021, **89**, 1, DOI: [10.3390/scipharm89010001](https://doi.org/10.3390/scipharm89010001).
- 7 N. Songnaka, M. Lertcanawanichakul, A. M. Hutapea, S. Krobthong, Y. Yingchutrakul and A. Atipairin, Purification and characterization of novel anti-MRSA peptides produced by *Brevibacillus* sp. SPR-20, *Molecules*, 2022, **27**, 8452, DOI: [10.3390/molecules27238452](https://doi.org/10.3390/molecules27238452).
- 8 P. P. Nugrahadi, W. L. J. Hinrichs, H. W. Frijlink, C. Schöneich and C. Avanti, Designing formulation strategies for enhanced stability of therapeutic peptides in aqueous solution: a review, *Pharmaceutics*, 2020, **15**, 935, DOI: [10.3390/pharmaceutics15030935](https://doi.org/10.3390/pharmaceutics15030935).
- 9 A. K. Tiwari, V. Gajbhiye, R. Sharma and N. K. Jain, Carrier mediated protein and peptide stabilization, *Drug Deliv.*, 2010, **17**, 605–616, DOI: [10.3109/10717544.2010.509359](https://doi.org/10.3109/10717544.2010.509359).
- 10 W. Gao, D. Vecchio, J. Li, J. Zhu, Q. Zhang, V. Fu, J. Li, S. Thamphiwatana, D. Lu and L. Zhang, Hydrogel containing nanoparticle-stabilized liposomes for topical antimicrobial delivery, *ACS Nano*, 2014, **8**, 2900–2907, DOI: [10.1021/nn500110a](https://doi.org/10.1021/nn500110a).
- 11 H. Schreier and J. Bouwstra, Liposomes and niosomes as topical drug carriers: dermal and transdermal drug delivery, *J. Controlled Release*, 1994, **30**, 1–15, DOI: [10.1016/0168-3659\(94\)90039-6](https://doi.org/10.1016/0168-3659(94)90039-6).
- 12 A. Dashti, A. R. Karamibonari, A. R. Farahpour and Z. G. Tabatabaei, Topical effectiveness of eugenol phytosome/chitosome hydrogels on the healing process of infected excision wounds, *Colloids Surf. A*, 2024, **678**, 133482, DOI: [10.1016/j.colsurfa.2024.133482](https://doi.org/10.1016/j.colsurfa.2024.133482).
- 13 A. H. Elmaidomy, S. A. Mohamad, M. Abdelnaser, R. Yahia, F. A. Mokhtar, F. Alsenani, M. Y. Badr, S. Y. Almaghrabi, F. H. Altemani, M. A. Alzubaidi, E. A. Saber, M. A. Elrehany, U. R. Abdelmohsen and A. M. Sayed, *Vitis vinifera* leaf extract liposomal carbopol gel preparation's potential wound healing and antibacterial benefits: *in vivo*, phytochemical, and computational investigation, *Food Funct.*, 2023, **14**, 7156, DOI: [10.1039/d2fo03212k](https://doi.org/10.1039/d2fo03212k).
- 14 P. Das, S. Ganguly, A. Saravanan, S. Margel, A. Gedanken, S. Srinivasan and A. R. Rajabzadeh, Naturally derived carbon dots *in situ* confined self-healing and breathable hydrogel monolith for anomalous diffusion-driven phytomedicine release, *ACS Appl. Bio Mater.*, 2022, **5**, 5617–5633, DOI: [10.1021/acsabm.2c00664](https://doi.org/10.1021/acsabm.2c00664).
- 15 P. Das, S. Ganguly, P. K. Marvi, M. Sherazee, S. R. Ahmed, X. Tang, S. Srinivasan and A. R. Rajabzadeh, Borophene based 3D extrusion printed nanocomposite hydrogel for



antibacterial and controlled release application, *Adv. Funct. Mater.*, 2024, **34**, 2314520, DOI: [10.1002/adfm.202314520](https://doi.org/10.1002/adfm.202314520).

16 G. Aizik, C. A. Ostertag-Hill, P. Chakraborty, W. Choi, M. Pan, D. V. Mankus, A. K. R. Lytton-Jean and D. S. Kohane, Injectable hydrogel based on liposome self-assembly for controlled release of small hydrophilic molecules, *Acta Biomater.*, 2024, **183**, 101–110, DOI: [10.1016/j.actbio.2024.05.044](https://doi.org/10.1016/j.actbio.2024.05.044).

17 R. Binaymotagh, F. H. Haghghi, L. Chronopoulou and C. Palocci, Liposome-hydrogel composites for controlled drug delivery applications, *Gels*, 2024, **10**, 284, DOI: [10.3390/gels10040284](https://doi.org/10.3390/gels10040284).

18 H. K. Mæhre, L. Dalheim, G. K. Edvinsen, E. V. Elvevoll and I. Jensen, Protein determination-method matters, *Foods*, 2018, **7**, 5, DOI: [10.3390/foods7010005](https://doi.org/10.3390/foods7010005).

19 P. Kesharwani, S. Md, N. A. Alhakamy, K. M. Hosny and A. Haque, QbD enabled azacitidine loaded liposomal nanoformulation and its *in vitro* evaluation, *Polymers*, 2021, **13**, 250, DOI: [10.3390/polym13020250](https://doi.org/10.3390/polym13020250).

20 Clinical and Laboratory Standards Institute, *Clinical and Laboratory Standards Institute in Methods for Dilution Antimicrobial Susceptibility Tests for Bacteria that Grow Aerobically*, Clinical and Laboratory Standards Institute, Wayne, PA, USA, 11th edn, 2018, pp. 15–52.

21 H. F. Goh and K. Philip, Purification and characterization of bacteriocin produced by *Weissella confusa* A3 of dairy origin, *Plos One*, 2015, **10**, e0140434, DOI: [10.1371/journal.pone.0140434](https://doi.org/10.1371/journal.pone.0140434).

22 N. Changsan, S. Sawatdee, R. Suedee, C. Chunhachaichana and T. Srichana, Aqueous cannabidiol  $\beta$ -cyclodextrin complexed polymeric micelle nasal spray to attenuate *in vitro* and *ex vivo* SARS-CoV-2-induced cytokine storms, *Int. J. Pharm.*, 2023, **640**, 123035, DOI: [10.1016/j.ijpharm.2023.123035](https://doi.org/10.1016/j.ijpharm.2023.123035).

23 D. Inoue, A. Yamashita and H. To, Development of *in vitro* evaluation system for assessing drug dissolution considering physiological environment in nasal cavity, *Pharmaceutics*, 2022, **24**, 2350, DOI: [10.3390/pharmaceutics14112350](https://doi.org/10.3390/pharmaceutics14112350).

24 A. Atipairin, C. Chunhachaichana, T. Nakpheng, N. Changsan, T. Srichana and S. Sawatdee, Development of a sildenafil citrate microemulsion-loaded hydrogel as a potential system for drug delivery to the penis and its cellular metabolic mechanism, *Pharmaceutics*, 2020, **12**, 1055, DOI: [10.3390/pharmaceutics12111055](https://doi.org/10.3390/pharmaceutics12111055).

25 N. Balekar, N. G. Katkam, T. Nakpheng, K. Jehtae and T. Srichana, Evaluation of the wound healing potential of *Wedelia trilobata* (L.) leaves, *J. Ethnopharmacol.*, 2012, **141**, 817–824, DOI: [10.1016/j.jep.2012.03.019](https://doi.org/10.1016/j.jep.2012.03.019).

26 Asean Guideline on Stability Study of Drug Product. Available at: <https://asean.org/wp-content/uploads/2018/01/25PPWG-ANNEX-7-iv-Final-ASEAN-Guideline-on-Stability-Study-Drug-Product-R2.pdf>, accessed September 2021.

27 S. Magréault, F. Jauréguy, E. Carbonnelle and J. R. Zahar, When and how to use MIC in clinical practice?, *Antibiotics*, 2022, **11**, 1748, DOI: [10.3390/antibiotics11121748](https://doi.org/10.3390/antibiotics11121748).

28 S. Shah, G. Barton and A. Fischer, Pharmacokinetic considerations and dosing strategies of antibiotics in the critically ill patient, *J. Intensive Care Soc.*, 2015, **16**, 147–153, DOI: [10.1177/1751143714564816](https://doi.org/10.1177/1751143714564816).

29 *Liposome Technology: Liposome Preparation and Related Techniques*, ed. G. Gregoriadis, CRC Press, Boca Raton, 3rd edn, 2006, vol. 1, DOI: [10.1201/9780849397264](https://doi.org/10.1201/9780849397264).

30 T. Kumarage, N. B. Morris and R. Ashkar, The effects of molecular and nanoscopic additives on phospholipid membranes, *Front. Phys.*, 2023, **11**, 1251146, DOI: [10.3389/fphy.2023.1251146](https://doi.org/10.3389/fphy.2023.1251146).

31 M. Danaei, M. Dehghankhodd, S. Ataei, F. H. Davarani, R. Javanmard, A. Dokhani, S. Khorasani and M. R. Mozafari, Impact of particle size and polydispersity index on the clinical applications of lipidic nanocarrier systems, *Pharmaceutics*, 2018, **10**, 57, DOI: [10.3390/pharmaceutics10020057](https://doi.org/10.3390/pharmaceutics10020057).

32 H. Nsairat, D. Khater, U. Sayed, F. Odeh, A. A. Bawab and W. Alshaer, Liposomes: structure, composition, types, and clinical applications, *Heliyon*, 2022, **8**, e09394, DOI: [10.1016/j.heliyon.2022.e09394](https://doi.org/10.1016/j.heliyon.2022.e09394).

33 S. Shaker, A. R. Gardouh and M. M. Ghorab, Factors affecting liposomes particle size prepared by ethanol injection method, *Res. Pharm. Sci.*, 2017, **12**, 346–352, DOI: [10.4103/1735-5362.213979](https://doi.org/10.4103/1735-5362.213979).

34 P. Sakdiset, F. J. Arce, G. L. See, S. Sawatdee and A. SaeYoon, Preparation and characterization of lidocaine HCl-loaded proniosome gels with skin penetration enhancers, *J. Drug Deliv. Sci. Technol.*, 2023, **86**, 104639, DOI: [10.1016/j.jddst.2023.104639](https://doi.org/10.1016/j.jddst.2023.104639).

35 U. D. Shihhare, D. U. Ambulkar, V. B. Mathur, K. P. Bhusari and M. D. Godbole, Formulation and evaluation of pentoxifylline liposome formulation, *Dig. J. Nanomater. Biostruct.*, 2009, **4**, 631–637.

36 K. Ullmann, G. Lenewelt and H. Nirschl, How to achieve high encapsulation efficiencies for macromolecular and sensitive APIs in liposomes, *Pharmaceutics*, 2021, **13**, 691, DOI: [10.3390/pharmaceutics13050691](https://doi.org/10.3390/pharmaceutics13050691).

37 *Liposomes Method and Protocols: Pharmaceutical Nanocarriers*, ed. V. Weissig, Humana Totowa Press, NJ, 2010, vol. 1, DOI: [10.1007/978-1-60327-360-2](https://doi.org/10.1007/978-1-60327-360-2).

38 Z. Németh, I. Csóka, R. S. Jazani, B. Sipos, H. Haspel, G. Kozma, Z. Kónya and D. G. Dobó, Quality by design-driven zeta potential optimisation study of liposomes with charge imparting membrane additives, *Pharmaceutics*, 2022, **14**, 1798, DOI: [10.3390/pharmaceutics14091789](https://doi.org/10.3390/pharmaceutics14091789).

39 P. J. Kadu, S. S. Kushare, D. D. Thacker and S. G. Gattani, Enhancement of oral bioavailability of atorvastatin calcium by self-emulsifying drug delivery systems (SEDDS), *Pharm. Dev. Technol.*, 2011, **16**, 65–74, DOI: [10.3109/10837450903499333](https://doi.org/10.3109/10837450903499333).

40 E. D. Castañeda-Reyes, M. J. Perea-Flores, G. Davila-Ortiz, Y. Lee and E. G. Mejia, Development, characterization and use of liposomes as amphiphatic transporters of bioactive compounds for melanoma treatment and reduction of skin inflammation: a review, *Int. J. Nanomed.*, 2020, **15**, 7627–7650, DOI: [10.2147/IJN.S263516](https://doi.org/10.2147/IJN.S263516).



41 R. R. Kumal, H. Nguyenhuu, J. E. Winter, R. L. McCarley and L. H. Haber, Impacts of salt, buffer, and lipid nature on molecular adsorption and transport in liposomes as observed by second harmonic generation, *J. Phys. Chem. C*, 2017, **121**, 15851–15860.

42 V. Peikov, T. Radeva, S. P. Stoylov and H. Hoffmann, Electric light scattering from polytetrafluorethylene suspensions II. influence of dialysis, in *Trends in Colloid and Interface Science X*, ed. C. Solans, M. R. Infante and M. J. García-Celma, Steinkopff, Heidelberg, Germany, 1996, pp. 64–67, DOI: [10.1007/BFB01157540](https://doi.org/10.1007/BFB01157540).

43 G. M. Shashidhar and B. Manoher, Nanocharacterization of liposomes for the encapsulation of water soluble compounds from *Cordyceps sinensis* CS1197 by a supercritical gas anti-solvent technique, *RSC Adv.*, 2018, **8**, 34634, DOI: [10.1039/C8RA07601D](https://doi.org/10.1039/C8RA07601D).

44 D. G. Metcalf, M. Haalboom, P. G. Bowler, C. Gamerith, E. Sigl, A. Heinzle and M. W. M. Burnet, Elevated wound fluid pH correlates with increased risk of wound infection, *Wound Med.*, 2019, **26**, 100166, DOI: [10.1016/j.wndm.2019.100166](https://doi.org/10.1016/j.wndm.2019.100166).

45 H. Lambers, S. Piessens, A. Bloem, H. Pronk and P. Finkel, Natural skin surface pH is on average below 5, which is beneficial for its resident flora, *Int. J. Cosmet. Sci.*, 2006, **28**, 359–370, DOI: [10.1111/j.1467-2494.2006.00344.x](https://doi.org/10.1111/j.1467-2494.2006.00344.x).

46 P. Sim, X. L. Strudwick, Y. Song, A. J. Cowin and S. Garg, Influence of acidic pH on wound healing *in vivo*: a novel perspective for wound treatment, *Int. J. Mol. Sci.*, 2022, **23**, 13655, DOI: [10.3390/ijms232113655](https://doi.org/10.3390/ijms232113655).

47 D. L. Pavia, G. M. Lampman and G. S. Kriz, Chapter 2 Infrared Spectroscopy, in *Introduction to Spectroscopy: A Guide for Students of Organic Chemistry*, Thomson Learning Inc., Chicago, IL, USA, 2001, pp. 13–101.

48 S. Peers, A. Montembault and C. Ladavière, Chitosan hydrogels for sustained drug delivery, *J. Control. Release*, 2020, **326**, 150–163, DOI: [10.1016/j.conrel.2020.06.012](https://doi.org/10.1016/j.conrel.2020.06.012).

49 M. Sugita, S. Sugiyama, T. Fujie, Y. Yoshikawa, K. Yanagisawa, M. Ohue and Y. Akiyama, Large-scale membrane permeability prediction of cyclic peptides crossing a lipid bilayer based on enhanced sampling molecular dynamics simulations, *J. Chem. Inf. Model.*, 2021, **61**, 3681–3695, DOI: [10.1021/acs.jcim.1c00380](https://doi.org/10.1021/acs.jcim.1c00380).

50 A. Billard, L. Pourchet, S. Malaise, P. Alcouffe, A. Moutembault and C. Ladavière, Liposome-loaded chitosan physical hydrogel: toward a promising delayed-release biosystem, *Carbohydr. Polym.*, 2015, **115**, 651–657, DOI: [10.1016/j.carbpol.2014.08.120](https://doi.org/10.1016/j.carbpol.2014.08.120).

51 S. Moroni, G. Curzi, A. Aluigi, M. Tiboni, M. Vergassola, M. Saviano, L. Marchitto, S. Zucchi, L. Ragni and L. Casettari, Influence of permeability enhancers on *in vitro* peptides delivery through STRAT-M® membranes, *J. Drug Deliv. Sci. Technol.*, 2023, **89**, 104987, DOI: [10.1016/j.jddst.2023.104987](https://doi.org/10.1016/j.jddst.2023.104987).

52 O. Kapusta, A. Jarosz, K. Stadnik, D. A. Giannakoudakis, B. Barczynski and M. Barczak, Antimicrobial natural hydrogels in biomedicine: properties, applications, and challenges – a concise review, *Int. J. Mol. Sci.*, 2023, **24**, 2191, DOI: [10.3390/ijms24032191](https://doi.org/10.3390/ijms24032191).

53 J. Cui, Z. Wen, W. Zhang and W. Wu, Recent advances in oral peptide or protein-based drug liposomes, *Pharmaceutics (Basel)*, 2022, **15**, 1072, DOI: [10.3390/ph15091072](https://doi.org/10.3390/ph15091072).

54 V. G. S. S. Jyothi, R. Bulusu, B. V. K. Rao, M. Pranothi, S. Banda, P. K. Bolla and N. Kommineni, Stability characterization for pharmaceutical liposome product development with focus on regulatory considerations: an update, *Int. J. Pharm.*, 2022, **25**(624), 122022, DOI: [10.1016/j.ijpharm.2022.122022](https://doi.org/10.1016/j.ijpharm.2022.122022).

